Characterization of the EPF family of signaling peptides controlling stomatal development in monocots

Raman Jangra

A Thesis

in

The Department

of

Biology

Presented in Partial Fulfillment of the Requirements

for the Degree of Master of Science (Biology) at

Concordia University

Montreal, Quebec, Canada

May 2020

CONCORDIA UNIVERSITY
School of Graduate Studies

This is to certify that the thesis prepared

By: Raman Jangra

Entitled: **Characterization of the EPF family of signaling peptides controlling stomatal development in monocots**

and submitted in partial fulfillment of the requirements for the degree of

Master of Sciences (Biology)

complies with the regulations of the University and meets the accepted standards with respect to originality and quality.

Signed by the final examining committee:

_____ Chair
Dr. Patrick Gulick

_____ External Examiner
Dr. Vladimir Titorenko

_____ Examiner
Dr. Selvadurai Dayanandan

_____ Examiner
Dr. Madoka Gray-Mitsumune

_____ Supervisor
Dr. Jin Suk Lee

Approved by: _____
Dr. Robert Weladji, Graduate Program Director

_____
André G. Roy, Dean of Faculty of Arts and Science

Date _____

Abstract

Characterization of the EPF family of signaling peptides controlling stomatal development in monocots

Raman Jangra, M.Sc.

Stomata are pores on plant epidermis which control water and gas exchanges between plants and the atmosphere. These two processes are very crucial for adaptation against environmental changes and photosynthesis process which increases biomass of a plant. As such, proper density and distribution of stomata are critical for plant growth and survival. In *Arabidopsis*, several Epidermal Patterning Factor (EPF) family members of small cysteine-rich peptides have been discovered as important signaling molecules that possess diverse functions in controlling plant development, including stomatal patterning and differentiation. EPF1 and EPF2, released from stomatal precursor cells, enforces stomatal spacing divisions and inhibits initiation of stomatal cell lineage, respectively. They are known as negative regulators of stomata development. STOMAGEN/EPFL9, on the other hand, being a positive regulator promotes stomatal differentiation in the epidermis and expressed in the underlying mesophyll tissues. Although much is known about Dicots' EPFs, how EPF peptides control different stomatal patterns and morphologies exist in grasses remains unclear.

In this study, we searched for stomatal EPF homologs in other agriculturally important cereal crops using a bioinformatics followed by functional genomics studies. Our phylogenetic analysis revealed that there are genes encoding putative EPFs including stomatal EPFs, EPF1, EPF2, and STOMAGEN, in each of the grass species examined. To understand the roles of EPF peptides in grass stomatal development, we generated estradiol inducible overexpression lines for both wheat and *Brachypodium EPF1*, *EPF2* and *STOMAGEN* homologous genes in *Arabidopsis*. It resulted in identification of antagonistic stomatal ligands, which are duplicated ortholog of *Arabidopsis* AtEPF2 and AtSTOMAGEN peptides, in the wheat and *Brachypodium.*

We further investigated the behavior of *AtEPF1/2*-like genes from wheat and *Brachypodium* in the regulation of epidermal development by analyzing cross-species complementation studies followed by phenotypic effects of exogenously applied bioactive grass EPF peptides on *Brachypodium* wild type seedlings, Bd21-3. Application of bioactive BdEPF1/2 peptides inhibited

the stomatal initiation process in Bd21-3, whereas BdSTOMAGEN application promoted stomatal development in Bd21-3, resulting in an epidermis with clustered stomata.

Overall, the present study furthers our knowledge on conserved EPF peptides which controls different stomatal patterns that exist in nature and provides putative strategies to improve crop productivity by using plant-derived antagonistic peptides that optimize stomatal density on plant epidermis.

Acknowledgements

I would like to extend my profound regards and deep sense of gratitude to my supervisor, Dr. Jin Suk Lee for her prudent guidance, encouragement and constructive suggestions throughout. Her infinite capacity for hard work will always be an illuminating light to guide me in all my academic pursuits in future too. I am indebted to her timely advice, noble counseling and for providing the necessary facilities during my study.

With an overwhelming and genuine sense of obligations, I would like to thank my committee members Dr. Madoka Gray-Mitsumune and Dr. Selvadurai Dayanandan for their affectionate behavior, guidance and help.

I want to express my great appreciation to our collaborators Dr. Patrick Gulick and his lab members for providing a very important piece of data to carry out this research.

I would like to give a very special thanks to all members of my lab for their cooperation and encouragement at various stages of my research work. I am very grateful for their friendship and support, and for creating a cordial working environment.

I wish to acknowledge the help and constant support provided by Chris for all imaging and analysis processes and for being patient throughout.

I express my deepest sense of gratitude that I owe to my loving parents and siblings for their encouragement and motivation throughout to provide me the best of everything in life. They always boosted my zeal and strength to go ahead in completion of my work.

This journey would have never started without the encouragement and help of my friends who were always there to make me smile. Saying Thank you is not enough to express unconditional love, support and companionship I got from my friends. In every aspect, you guys made my life better everyday.

The warmth showered upon me through every handshake, every smile and many times through unsaid words are heartily acknowledged. Lastly, I am thankful to all those who have helped me directly or indirectly.

Table of Contents

List of Figures

List of Tables

List of Abbreviations

GMC	Guard Mother Cell
GC	Guard Cell
MMC	Meristemoid Mother Cell
SLGC	Stomatal Lineage Ground Cell
NGC	Non-Guard Cell
SMC	Subsidiary Mother Cell
bHLH	Basic helix-loop-helix
cDNA	Complementary DNA
Col	Columbia
DNA	Deoxyribonucleic Acid
Erf	Erecta Receptor Family
ERL1	ERECTA-Like 1
ERL2	ERECTA-Like 2
GFP	Green Fluorescent Protein
MS	Murashige and Skoog
PC	Pavement Cells
PCR	Polymerase Chain Reaction
RNA	Ribonucleic Acid
RNAi	RNA interference
TBO	Toluidine Blue O
WT	Wild Type

EPF	Epidermal Patterning Factor
EPFL	Epidermal Patterning Factor Like
CDS	Coding Sequence
KO	Knock Out
RT	Room Temperature
OE	Overexpression/Over Expressed
mRNA	Messenger RNA
AtEPF1	*Arabidopsis thalliana* Epidermal Patterning Factor 1
AtEPF2	*Arabidopsis thalliana* Epidermal Patterning Factor 2
AtSTOMAGEN	*Arabidopsis thalliana* Epidermal Patterning Factor-Like 9
BdEPF1	*Brachypodium distachyon* Epidermal Patterning Factor 1
BdEPF2	*Brachypodium distachyon* Epidermal Patterning Factor 2
BdSTOMAGEN-1	*Brachypodium distachyon* Epidermal Patterning Factor Like 9-1
BdSTOMAGEN-2	*Brachypodium distachyon* Epidermal Patterning Factor Like 9-2
TaEPF1	*Triticum aestivum* Epidermal Patterning Factor 1
TaEPF2	*Triticum aestivum* Epidermal Patterning Factor 2
TaSTOMAGEN-1	*Triticum aestivum* Epidermal Patterning Factor Like 9-1
TaSTOMAGEN-2	*Triticum aestivum* Epidermal Patterning Factor Like 9-2
MBdEPF1	Mature *Brachypodium distachyon* Epidermal Patterning Factor 1
MBdEPF2	Mature *Brachypodium distachyon* Epidermal Patterning Factor 2
MBdSTOMAGEN-1	Mature *Brachypodium distachyon* Epidermal Patterning Factor Like 9-1

1. Introduction

Cereals cover more than half of total food production, and among grasses, only maize, wheat, and rice together contribute to more than 75% of total world's annual grain production (FAO, 2017). Wheat and barley, known as small grain crops, are major source of food, forage and feed worldwide (Scholthof *et al.*, 2018). Wheat (*Triticum aestivum* L.) belongs to Poaceae family which also comprises other most important cereal crops including sorghum, maize, rice, millet and barley (Briggle and Reitz, 1963).

Wheat is one of the world's major food crops and according to recent FAO data, world's annual wheat production in 2019/2020 numbered to nearly 765.41 million metric tons (FAO, 2020). Wheat is also considered as one of the most staple crops for more than 33% of entire population and possesses more calorific and protein value as compared to other grain crops (Haleem *et al*., 1998; Adams *et al*., 2002; Shewry, 2007). Wheat provides 14.70% of the protein, 55% of the carbohydrate and 20% of the calories consumed globally particularly in developing countries. Altogether, wheat is nutritious, easy to store & ship and can be processed into various types of food (Breiman and Graur, 1995; Kumar *et al*., 2011). Normally, consumption of wheat is more than any other cereal crop (Singh and Singh, 2007). Most of the world's bread wheat is produced by Northern India, Northern China, Northern USA and neighboring areas in Latin America, Europe, Canada, Russia and Africa (Kole, 2006). In the present-day farming, bread wheat (*Triticum aestivum*) is broadly cultivated everywhere throughout the world, representing 95% of total wheat grown, and durum wheat (*Triticum durum*) constitutes the remaining 5% of total annual wheat production (Shewry, 2009). At present, a total of around 4000 spring or winter wheat varieties are cultivated all around the world (Posner, 2000).

However, with an estimate of surging world population to 9 billion by 2050 (Godfray *et al*., 2010), food shortage and water scarcity will become a severe problem all around the world. In addition to this, drought conditions, lowering of ground water levels and desertification is also going to predominant in upcoming 4-6 decades (IPCC, 2014). Therefore, investigators must find a way to develop water-efficient cereal crops with better health and yield chartacteristics (Hepworth *et al.*, 2017).

1.1 Why do we need to study stomatal development?

Since the structure of plant organs are closely related to their function, understanding their structure is important for improvement of plants to function optimally under various environmental conditions (Jarvis and Mansfield, 1981). It has been reported that in most plants including major crops, majority of water is being evaporated through stomata (Abrash and Gil, 2018). Stomata is a vital part for plants, being the interface between internal plant tissues and outer environment. Stomata is a tiny pore surrounded by two kidney (in dicots) or dumbbell shaped cells (in monocots) known as guard cells and involved in in two very crucial processes i.e. regulation of transpiration process (water vapor exchange) by closing and opening of stomata and photosynthesis (gaseous exchange) in which stomata typically open in response to sunlight exposure, in order to facilitate the uptake of CO_2 and release of oxygen. Normally, two stomata are one epidermal pavement cell apart from each other (Sachs 1991; Serna *et al*., 2002) so they can exchange water and gas properly. Stomata also plays an imperative part within the direction of plant growth and development, which is accomplished by the opening or closing of the stomatal pores (Casson and Gray, 2007; Bergmann and Sack, 2007; Colcombet and Hirt, 2008).

Although, plants of grass family provide the majority of world's food supply, many aspects of their growth, development and physiology, including stomatal development are less understood than those of the model dicot plant species. So, it is very crucial to explore grass stomatal development in detail, so that advanced crops with more sustainability to a variety of environmental conditions can be generated. In addition, it is very clear that stomatal number and density plays an important role in plant growth and development and alteration of stomatal density can be a major player in this path as it is directly related to plant growth and productivity. Therefore, in order to generate drought resistance crops with better productivity and WUE, it is crucial to understand how stomatal initiation and differentiation takes place in monocots.

1.2 Stomatal development

Stomata formation and patterning in dicots and grasses are different. To begin with, stomata in dicots possess two kidney shape guard cells and they are randomly scattered throughout the leaf epidermis. Whereas in grasses which represents a clade of monocots, stomata are of dumb-bell shape, flanked by two subsidiary cells and instead of oriented randomly, leaves of grasses have specific parallel stomatal cell files (Croxdale, 1998) in which stomatal differentiation starts from base towards tip **(Figure 1)** (Raissig *et al.,* 2017). Thus, one interesting question arise from this comparison is how different stomatal patterns and morphologies can be generated in the monocot crops, which may inform agricultural practices to improve crop biomass and water-use efficiency.

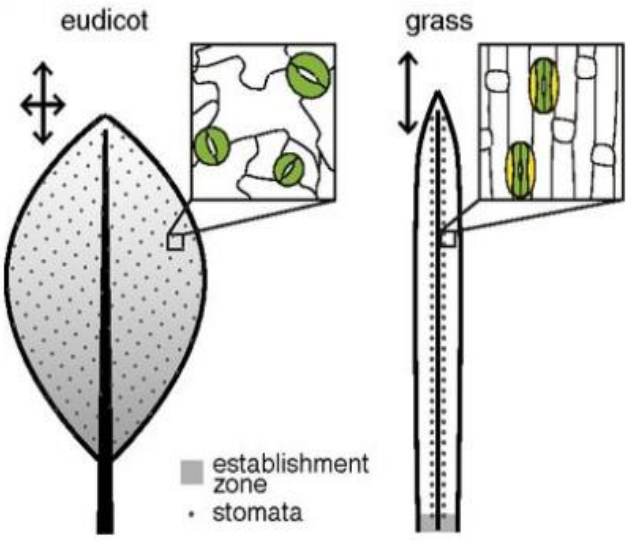

Figure 1. Comparison of stomatal structure and pattern in eudicot and grass leaves

Grasses exhibit a longitudinal gradient of development with divisions restricted to the leaf base and differentiation toward tip (Right). In Eudicot leaves, the stomata are randomly oriented and the stomatal stem cell populations are dispersed throughout the epidermis tip (Left). Image is adapted from Raissig *et al.*, 2017.

1.2.1 Stomata developmental process in model dicot (*Arabidopsis thaliana*)

Arabidopsis thaliana is considered as model dicotyledonous plant and being used for various plant related research due to many reasons. First, it has a fully sequenced small genome (114.5 Mb/125 Mb total) which makes this plant very easy to use for research purposes. In addition, it is a self-fertilizing plant with a short life cycle and can be easily manipulated by *Agrobacterium* mediated transformation process (TAIR). Stomata in *Arabidopsis* are characterized as epidermal pores flanked by two kidneys shaped (Raschke, 1979) guard cells (GCs) and all other neighboring cells are known as pavement cells.

Stomatal production in *Arabidopsis* requires several asymmetric cell divisions and a single symmetric cell division. Stomatal formation starts from a set of precursor cells called as protodermal cells which undergo asymmetric divisions and give rise to meristemoid mother cells (MMCs). These MMCs have stem cells like properties which means they are capable of regenerating themselves. Subsequently, MMCs undergo asymmetric division to produce two new cells that follow different paths **(Figure 2)**. The smaller triangular cell is a meristemoid that either differentiates into oval shaped guard mother cell (GMC), which subsequently undergoes symmetric division and differentiates into mature guard cells (GCs), or undergoes 1 to 3 amplifying divisions first before producing GMC (Bergmann and Sack, 2007; Nadeau and Sack, 2002a; Pillitteri and Torii, 2012). Neighboring cells can also divide asymmetrically to produce additional mersitemoids known as satellite meristemoid which is critical for proper stomatal patterning. (Larkin *et al*., 1997). Thus, during the growth of the epidermal cells, meristemoids may arise adjacent to GCs or other meristemoids. This meristemoid can retain stomatal cell fate but the next asymmetric division would be oriented away from the pre-existing stomatal cell resulting in new meristemoid separated from the stomata by a pavement cell (Geisler *et al*., 2000). In contrast, the larger daughter cell, which is called the stomatal-lineage ground cell (SLGC), undergoes terminal differentiation into a pavement cell (Casson and Gray, 2007).

The cell fate transitions during stomatal development are controlled by sequential action of three closely related basic helix loop helix (bHLH) transcriptional factors; SPEECHLESS (SPCH), MUTE and FAMA (Ohashi-Ito and Bergmann, 2006; MacAlister *et al*., 2007; Pillitteri *et al*., 2007; Bhave *et al*., 2009; Serna, 2009; Gudesblat *et al*., 2012). Two additional redundant bHLH proteins,

AtICE1 and AtSCRM2 are known to constitutively expressed in stomatal lineage and promotes cellular transitions during stomatal development by heteromerization with SPCH, MUTE and FAMA (Kanaoka *et al*., 2008). *SPCH* is expressed in MMC and controls entry into initial asymmetric cell divisions. That is why *spch* mutant results into an epidermis composed of only pavement cells (MacAlister *et al*., 2007). Second cell state transition from merisremoid to GMC requires *MUTE* expression and its loss of function mutant, *mute* results into meristemoid with multiple division (4-6 divisions) (Pillitteri *et al*., 2007). FAMA is required for the last cell state transition from GMC to GC. Consequently, cells failed to express *FAMA* results into an epidermal phenotype of abnormally divided guard mother cells that fail to differentiate into guard cells (Ohashi-Ito and Bergmann, 2006). Cell-cell communication specifying stomatal patterning is very important for proper stomatal distribution in plants and this is is achieved by recognition of cystine rich EPIDERMAL PATTERNING FACTOR (EPF)/EPF-LIKE (EPFL) family members by three leucine-rich repeat receptor kinases (LRR-RKs) ERECTA (ER)-family receptors, ER, ERL1 and ERL2, and one LRR receptor-like protein, TOO MANY MOUTHS (TMM) (Hara *et al*., 2007, 2009; Hunt and Gray, 2009; Nadeau and Sack, 2002: Shpak *et al*., 2005). These receptor-ligand interactions are followed by activation of a downstream MAPK cascade that involves (YDA), MKK4/5 and MPK3/6 (Bergmann *et al*., 2004; Wang *et al*., 2007).

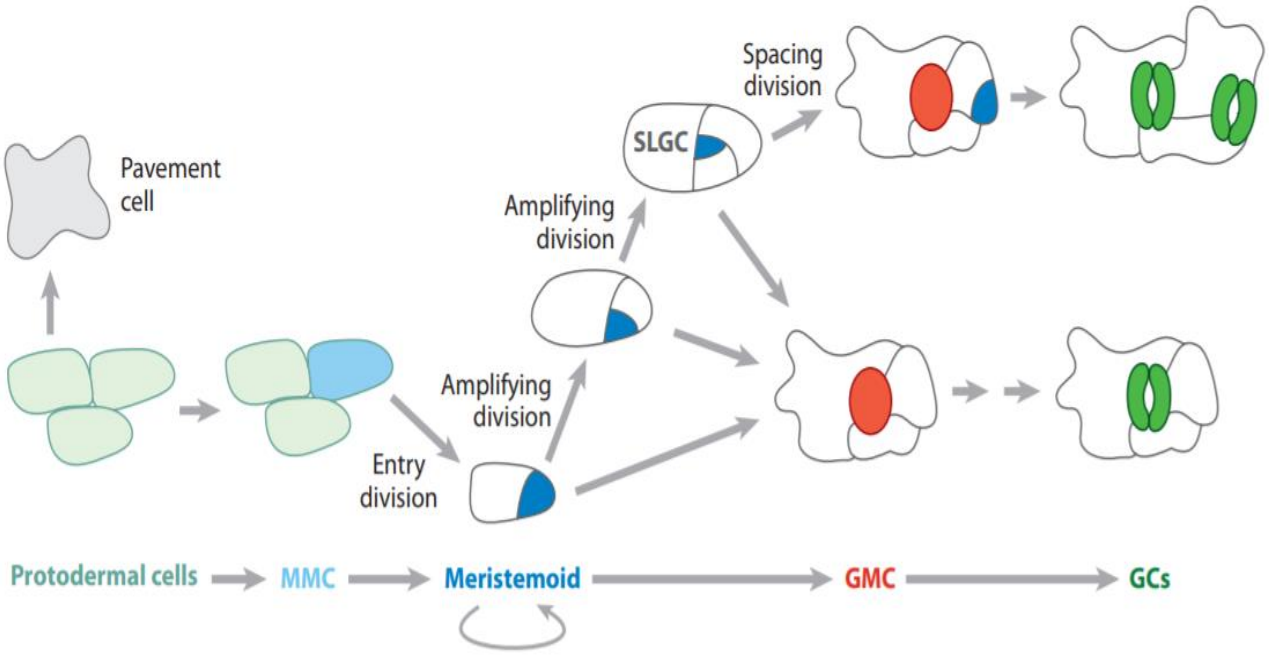

Figure 2. Stomatal development in *Arabidopsis thaliana*

In *Arabidopsis thaliana*, a population of protodermal cells (light green) undergo changes and convert into MMCs (Meristemoid Mother Cells) (light blue) which further asymmetrically divide into 2 cells, smaller cell known as meristemoid and larger cell known as SLGC. Later, meristemoid (dark blue) converts into Guard Mother Cell (GMC) (red) which finally divides symmetrically into two guard cells (GCs). SLGC can either convert into pavement cells or further divide to form a satellite meristemoid (dark blue). Adapted from Pillitteri and Torii, 2012.

1.2.2 Stomata developmental process in monocots

In monocots, there is a total four-cell stage known as stomatal complex with two dumbbell shaped guard cells flanked by two subsidiary cells. This subsidiary cell is known to be very critical for opening of stomatal pore by regulating guard cells expansion (Pillitteri and Dong, 2013).

In grasses, stomatal initiation and differentiation process takes place only in specific cells files which has preestablished fate of stomatal rows **(Figure 3)**. Stomatal differentiation starts from the base of leaf by some stomatal precursor cells which undergo one asymmetric division. Resulting small daughter cell is known as guard mother cell (GMC) and other big cell terminate as pavement cells. Afterwards, signals are being send by GMCs and perceived by neighboring cells in adjacent rows, resulting of which, they start dividing asymmetrically towards GMCs forming subsidiary mother cells (SMC). It has been shown that two specific plasma membrane proteins of SMC, PAN1 and PAN2, leucine-rich repeat–receptor-like kinase (LRR-RLK) receive signals from GMC and start dividing asymmetrically which ultimately matures as subsidiary cells (SC) (Smith *et al*., 2012). During stomatal development in maize, these two LRR-RLKs stimulates the polarization of SMC divisions toward the neighbour GMCs. Individual loss of function mutants *pan1* and *pan2* results into abnormal asymmetric cell division resulting into defected SC patterning (Gallagher and Smith, 2000; Smith *et al*., 2012). Following SC formation, GMCs divide once symmetrically and differentiate into two dumbbell shaped guard cells (Gallagher and Smith, 2000) flanked by two subsidiary cells, which ultimately perform gas and water exchange in grasses (Raissig *et al.*, 2016).

Availability of full genome sequences and recent advancements of sophisticated genetic and molecular techniques has allowed scientists to explore crucial genes involved in several plant developmental pathways in cereal crops, such as rice (*Oryza sativa*) and maize (*Zea mays*) (Jackson, 2016; Portwood *et al*., 2019). There have been some initial studies about monocot stomatal developmental process in maize, rice, barley and model monocot *Brachypodium distachyon* in past 10 years (Liu *et al.,* 2009; Raissig *et al*., 2017; Hepworth *et al.,* 2017; Caine *et al*., 2018; Wang *et al*., 2019). It also allows further analysis of conservation of genes in different species which could be important in stomatal patterning and/or differentiation processes (Peterson *et al.*, 2010). But our knowledge of various genes involved in different cereal's stomatal

development is still very diminutive Therefore, controlling or manipulating stomatal density can give rise to a new era crop with less water consumption and better yield.

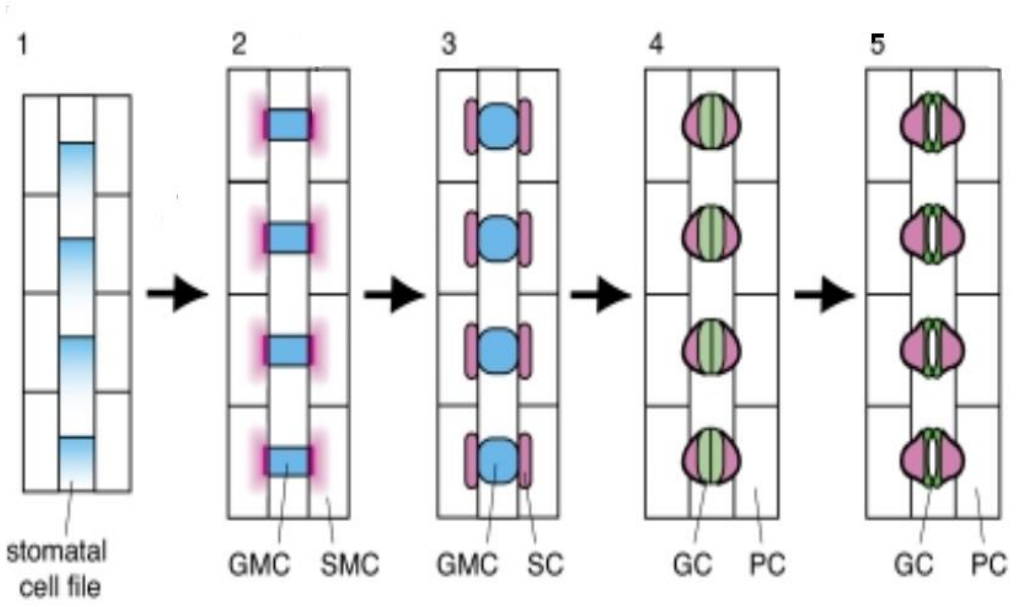

Figure 3. Stomatal development in grasses

(1) In early developmental stages, stomatal cell files are established which further divide asymmetrically into GMC (blue) (2). Mature GMC (blue) (3) convert into GC (light green) (4) after recruiting subsidiary cells (SC; pink), arises from subsidiary Mother Cells (SMCs; pink area) (2) which surrounds GMCs. Finally, dumbbell shaped stomata (dark green), flanked by two subsidiary cells are formed (5). Adapted from Peterson *et al.*, 2010.

1.3 Peptide signaling

1.3.1 Epidermal Patterning Factor (EPF) ligands

The EPF/EPFL signaling peptides are a part of superfamily of cysteine rich peptides (with intramolecular disulfide bonds formed by six or eight conserved carboxy-terminal cysteines). EPFs possess a N-terminal signal sequence which is being cleaved upon maturation and 6-8 cysteine residues on C-terminal are responsible for intramolecular disulfide linkage (Kondo *et al.,* 2010). These bonds are very crucial for proper folding and activity of peptide (Ohki *et al*., 2011). The functional diversity of the EPF family peptides can be attributed to the conservation of cysteines, which form a long loop with enormous sequence variety as well as variety in length between the fourth and fifth conserved cysteines (Kondo *et al.*, 2010).

EPF/EPFL, small secretory peptides, are conserved in various land plant species. The EPF ligands family (EPFf) is composed of 11 members (EPF1, EPF2 and EPFL1-9) which are indulged in multiple plant developmental processes in *Arabidopsis* (Hara *et al.,* 2007; Hara *et al.,* 2009; Hunt and Gray, 2009; Rowe and Bergmann, 2010; Peterson *et al*., 2010; Torii, 2012; Richardson and Torii, 2013; Pilliteri and Dong, 2013). Based on sequence similarity, EPFL peptides are categorized into 4 different subdivisions (Takata *et al*., 2013). EPFL8 peptide lies in one subgroup, whereas EPF1, EPF2 and EPFL7 comes under another subgroup which is closely related to third subgroup holding STOMAGEN alone. The last subgroup involves rest of 3 EPFs; EPFL1, EPFL2 and EPFL3 (Bessho-Uehara *et al*., 2016; Tameshige *et al.,* 2016).

All lad plants use EPFs as they emit signals for their respective receptors to regulate various plant developmental stages (Dohlman and Thorner, 2001; Gao and Guo, 2012; Karamboulas and Ailles, 2012; Pilliteri and Dong, 2013). Some of these peptides are known to emit signals which are perceived by multifunctional ERECTA family receptors (ERfs) and regulate ERf activity (Torii *et al*., 1996; Shimada *et al*., 2011) in model dicot plant *Arabidopsis*.

Some of these EPFs have been well thought-out in detail up until now. Two of them, EPF1 and EPF2 are involved in early stages of stomatal differentiation and patterning and are negative regulators of stomatal development (Hara *et al*., 2007, 2009; Hunt and Gray, 2009). On the other

hand, STOMAGEN/EPFL9 controls stomata growth in underlaying mesophyll tissues in a positive manner development (Hunt *et al*., 2010; Sugano *et al*., 2010; Shimada *et al.,* 2011) **(Figure 4)**.

EPFL1 normally expresses in root apical meristem and hypocotyl epidermis in *Arabidopsis*. EPFL1 has also been characterized in some grain crop and scientists found out that a rice *EPFL1* ortholog is involved in awn elongation (Bessho-Uehara *et al*., 2016).

There have been some deep studies of EPFL2 ligand by using loss of function and overexpression studies and it has been shown that EPFL2 requires for growth of leaf teeth. It interacts with ERECTA and inhibits the auxin response at tip of tooth during tooth development process (Wang *et al*., 2016; Tameshige *et al.,* 2016). It was also hypothesised that this ligand is accountable for leaf margin shapes as *epfl2* mutant leaves possessed smooth edges leaves (Tameshige *et al.,* 2016). Both *EPFL1* and *EPFL2* expression has been reported in emerging embryos which shows their possible involvement in organ elongation same as EPFL4 and EPFL6 (Kosentka *et al.,* 2019).

Another EPFL ligand, EPFL4 have been known to work redundantly with EPFL6 and it helps in elongation of above ground tissues. EPFL4 and EPFL6 are chiefly expressed in the endodermis of developing inflorescence stems (Tameshige *et al.,* 2016; Kosentka *et al.,* 2019). According to scientists, a double *epfl4epfl6* mutant plant height were shorter with compact inflorescence as compare to wild-type showing that these genes contribute in inflorescence architecture in hypocotyl redundantly (Abrash *et al*., 2011; Uchida *et al*., 2012).

1.3.2 Stomatal EPFs

There are 3 EPFs involved in stomatal development process, i.e. EPF1 (At2g20875), EPF2 (At1g34245) and STOMAGEN (At4G12970) (Torii, 2012). Both EPF1 and EPF2 are known to have structure similarities with an additional disulfide bond (Takata *et al.*, 2013) and they are called as negative stomatal regulators. Both, *EPF1* and *EPF2* are expressed in the stomatal lineage explicitly. But their signals, which are received by their respective receptors are very specific and are not substitutable (Hara *et al*., 2009; Lee *et al*., 2012).

Loss of function *epf2* mutant results in excessive numbers of small stomatal-lineage cells and a surged number of stomata (Hara *et al*., 2009). Whereas *epf1* mutants have a phenotype of paired adjacent stomata in a non-parallel orientation (Hara *et al*., 2007). Upon overexpressing *EPF2* and *EPF1*, they show a phenotype of epidermis solely composed of pavement cells and many small arrested cells respectively. *EPF2* is mainly expressed in early stages in stomatal lineage, mainly in early precursors, MMCs and early meristemoids and EPF1 is produced by late meristemoid cells, GMCs and young guard cells (Hara *et al*., 2007; Hara *et al*., 2009; Hunt and Gray, 2009).

In initial stages of stomatal production, *EPF1* and *EPF2*, expressed by stomatal precursor cells (Hara *et al*., 2007, 2009; Hunt and Gray 2009) transmit signals which are sensed by extracellular LRR-RLK ERECTA family receptors. Transmembrane ERf receptors perceive signals from specific EPF ligand and form ligand-receptor pairs regulating different stages of proper stomata production and growth. Scientists have shown that ER-EPF2 and ERL1-EPF1 act as prime ligand-receptor pairs and they don't interact vice versa which define their specificity towards each other. ER-EPF2 regulates entry divisions and ERL1-EPF1 controls spacing divisions (Lee *et al*., 2012) which allow proper stomatal distribution.

Third stomatal ligand, STOMAGEN (45-amino-acid peptide with three intramolecular disulfide bonds) is chiefly expressed in underlaying mesophyll tissues which connect to outer environment through the pores of stomata (Kondo *et al*., 2010; Sugano *et al*., 2010). It acts as a positive regulator of stomatal development, which endorses stomatal differentiation (Hunt *et al*., 2010; Kondo *et al*., 2010; Sugano *et al*., 2010; Shimada *et al*., 2011). Overexpression of *STOMAGEN* results into a higher stomatal cell density and increased number of clustered stomata. On contrary, *STOMAGEN*

RNAi knockdown lines shows a phenotype having fewer stomata as compare to wild type (Sugano *et al*., 2010). To summarize, *Arabidopsis* EPF family of signaling peptides are very critical and involved in various biological process ranging from patterned stomatal differentiation to development of different plant organs in *Arabidopsis*. However, the function of EPF peptides in other agriculturally important crops remains elusive.

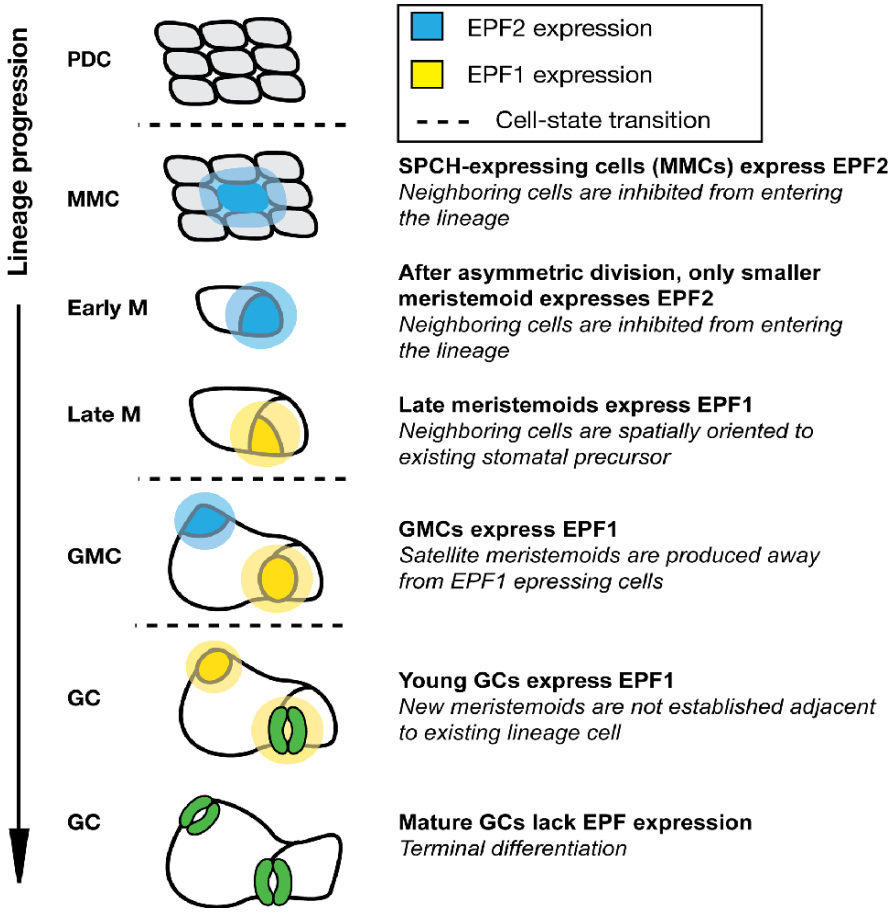

Figure 4. Early stage stomatal EPFs expression at different stages of stomata development
Protodermal cells expressing *SPCH*, secrete EPF2 (blue) and prevent neighboring cells from entering the stomatal lineage. The *EPF2*-expressing cell becomes a MMC and initiates asymmetric entry division. Late-stage meristemoids, GMCs and young GCs express *EPF1*, which spatially orients neighbor cells to existing stomatal precursors. Adapted from Pillitteri and Dong, 2013.

1.4 Objective and Hypothesis:

The present knowledge about various genes and molecular regulatory system involved in monocots' (especially cereal grasses) stomatal development process is limited. Discovering and characterizing different stomatal development related genes in monocots will enable us to gain insights into cell differentiation and use that information to develop crops with better water use efficiency and eventually improving plant productivity. Also, grain crops with increased stomatal density could absorb more atmospheric CO_2 and will serve as a good option for mitigating global warming. Therefore, the investigation of genes that control stomatal development will be highly valuable.

Based on previous studies, we recognize that stomatal patterning in *Arabidopsis* has arisen as a substantial model system for the study of molecular level regulation and genetics of cell differentiation, pattern formation in dicot plants. It involves different transcriptional factors, MAP kinases, signaling peptides and receptors. Among signaling peptides in *Arabidopsis* (dicot), three EPFs are mainly involved in controlling stomatal patterning and differentiation i.e. EPF1, EPF2, STOMAGEN. Identifying and characterizing such genes that can control and alter stomatal differentiation and density in monocots is valuable for enhancing agronomic productivity. Thus, we aim to investigate if:

- there are EPF homologous genes exist in cereal crops?
- they exist, then what functions do they possess as compared to well described stomatal EPFs in dicots plants?

To understand the roles of secreted EPF peptides in grass development, we searched for EPF homologs in major cereal crops and the grass model plant *Bracvhypodium distachyon* using sequence similarity based phylogenetic analysis followed by a series of functional genomics studies. We identified at least four grass EPF homologs of well-known *Arabidopsis* stomatal EPFs, AtEPF1, AtEPF2 and AtSTOMAGEN, that control grass stomatal development. Furthermore, using bioactive grass EPF peptides, we showed that despite plant species-specific differences in stomatal patterning, grasses initiate stomatal lineage using those four grass EPF peptides, which are duplicated orthologs of *Arabidopsis* EPF2 and STOMAGEN peptides. This finding emphasizes

that stomatal initiation in both plant species, dicots and monocots, needs precise regulation by both positive and negative peptide signals.

2. Material and Methods

2.1. Plant materials and growth conditions

Arabidopsis thaliana Columbia (Col) accession was used as wild type controls and following mutants and transgenic plants described previously - *epf1* (Hara *et al*., 2007), *epf2* (Hara *et al*., 2009), *proEst:EPF1*, *proEst:EPF2* (Lee *et al*., 2012) and *proEst:AtSTOMAGEN* (Lee *et al*., 2015) were used as experimental plants. Each transgene was introduced into Col and respective mutant background by *Agrobacterium*-mediated transformation. *Brachypodium* line Bd21-3 was used for mature peptide bioassays.

Seeds were surface sterilized by soaking with 1ml of sterilization solution {30% sodium hypochlorite (NaOCl), 0.19% triton X-100)} for 10 minutes on a rotary shaker, followed by 4-5 times washing with autoclaved double distilled water. After that, seeds were vernalized at 4^{o}C dark conditions for 2-3 days to perform all the phenotypic studies. Furthermore, seeds were plated on ½ Murashige and Skoog (MS) medium supplemented with 1% of sucrose and 0.68% agar (BiShop). To grow different transgenic seedlings, respective antibiotics with optimized concentration, were used in the ½ MS media plates. All seeds were grown in a standard growth chamber under following controlled conditions; 22°C temperature, 100 µmol m-2 s-1 light intensity and long-day cycle (18h light/6h dark). When needed, 5-6-day old *Brachypodium* seedlings and 10-day-old *Arabidopsis* seedlings were transferred to soil (2 black earth: 1 vermiculite: 1 peat moss) and grown at 22°C under the long-day condition (18h light/6h dark). In each soil pot, nine *Arabidopsis* seedlings were transplanted to maintain consistent growth conditions throughout the research work.

2.2 Phylogenetic analysis

Amino acid sequences of C-terminal mature peptide regions of the 11 EPF family members from *Arabidopsis* were used for searching in the Gene Bank and Phytozome databases for homologous genes in *Brachypodium distachyon*, *Triticum aestivum* (wheat), *Oryza sativa* (rice), *Hordeum vulgare* (barley), *Sorghum bicolor* (sorghum) and *Zea mays* (maize). The evolutionary history was

inferred by using the Maximum Likelihood method based on the Whelan And Goldman model (Whelan and Goldman, 2001). An initial tree for the heuristic search were obtained automatically by applying Neighbor-Joining and BioNJ algorithms to a matrix of pairwise distances estimated using a Jones Taylor Thornton (JTT) model, and then selecting the topology with higher log likelihood value. A discrete Gamma distribution was used to model evolutionary rate differences among sites (5 categories (+G, parameter = 0.6015)). The analysis involved 87 amino acid sequences. All positions with less than 95% site coverage were eliminated. That is, fewer than 5% alignment gaps, missing data, and ambiguous bases were allowed at any position. These procedures were performed using MEGA software (version 7.0) (Kumar *et al*., 2016).

2.3 Plasmid construction, generation and selection of transgenic plants

Plasmid construction: The following constructs were generated and used in this study: pJSL156 (BdEPF1 cDNA), pJSL151 (*proEst::BdEPF1*), pJSL155 and pJSL157 (BdEPF1 cDNA), pJSL158 (*proEst::BdEPF2*), pJSL148 (BdSTOMAGEN-1 cDNA), pJSL149 (*proEst:: BdSTOMAGEN-1*), pJSL185 (BdSTOMAGEN-2 cDNA), pJSL187 (*proEst:: BdSTOMAGEN-2*), pJSL171 (TaEPF1 cDNA), pJSL179 (*proEst:: TaEPF1*), pJSL173 (TaEPF2 cDNA), pJSL180 (*proEst:: TaEPF2*), pJSL177 (TaSTOMAGEN-1 cDNA), pJSL181 (*proEst:: TaSTOMAGEN-1*), pJSL188 (*proEst:: TaSTOMAGEN-2*), pJSL193 (EPF1 cDNA), pRJ14 (*proEPF1::nucGFP*), pRJ21 (*proEPF1::EPF1*), pRJ6 (*proEPF1::BdEPF1*), pRJ13 (*proEPF1::BdEPF2*), pRJ1 (*proEPF1::BdEPF2-GFP*), pRJ9 (*proEPF1::TaEPF1*), pRJ18 (*proEPF1::TaEPF2*), pJSL146 (*EPF2* promoter), pJSL194 (EPF2 cDNA), pRJ23 (*proEPF2::nucGFP*), pRJ22 (*proEPF2::EPF2*), pJSL175 and pRJ17 (*proEPF2::BdEPF1*), pRJ16 (*proEPF2::BdEPF2*), pJSL159 and pRJ5 (*proEPF2::BdEPF2*-GFP), pJSL190 and pRJ20 (*proEPF2::TaEPF1*), pRJ19 (*proEPF1::TaEPF2*), pJSL198 (pBAD:: MBdEPF1-6xHis), and pJSL199 (pBAD::MBdEPF2-6xHis). Plasmid pER8 (Zuo *et al*., 2000) was used for estradiol-inducible constructs and Gateway-cloning system (Invitrogen) was used to generate most constructs for the cross-species complementation studies. All details about the plasmids construction and primers used in this study are listed in Table 1 and 2.

Stable transgenic plants were generated using *Agrobacterium*-mediated transformation by the floral dipping method (Clough and Bent, 1998).

Agrobacterium mediated transformation: To perform this process, 1.5µl of plasmid DNA was used to transform *Agrobacterium* (GV3101 strain) competent cells with the cloned constructs. After introducing the DNA in ~50µl of GV3101 cells, the whole solution was transferred in prechilled glass cuvettes on ice. To perform electroporation, an electric shock was introduced using MicroPulsar Electroporator (Bio-Rad). Afterwards, 1ml of SOC media was added and tubes were incubated at 28°C for 1hr at 180 rpm followed by plating ~50µl of grown cells on LB media (1% NaCl, 1% Tryptone, 0.5% yeast extract in H_2O, pH 7.0) plates with appropriate bacterial selection marker. After 2days of appropriate incubation at 28°C, colonies of transformed *Agrobacteria* were cultured in liquid broth for further floral dipping.

Generation of transgenic plants: Floral dip method, as described by Clough and Bent (1998) was used for generation of *Arabidopsis* transgenic plants. As per method, 4-4.5ml of primary overnight grown GV3101 cells carrying transgene were used to inoculate 400ml of LB medium with selective antibiotic and Gentamycin and incubated at 28°C at 200 rpm for 1.5days. After appropriate growth, cells were centrifuged at 6000rpm for 20minutes. The resulting pellet was then resuspended in 400 ml of dipping solution containing 5% sucrose and 0.05% Silwett L-77. Plants with nearly 10cm inflorescences were inverted and only the bolted portion were dipped for 5seconds twice in dipping solution. After dipping, plants were covered with tray lid and kept overnight in dark at RT. Next Morning, domed plants were kept straighten in growth chamber and watered well. After 1-2 weeks of further growth, plants were kept in green house for drying and lastly, dried seeds were harvested.

Selection of transgenic plants: After harvesting, transgenic seeds were sowed on ½ MS plates supplemented with antibiotic, specific to that transgene selection. Transformants were selected as antibiotic-resistant seedlings with green leaves and firm roots and transplanted to get next generation seeds. More than 40 independents transgenic T1 or T2 lines per construct were screened and subjected to detailed phenotypic characterization.

2.4 DNA extraction, genotyping and PCR

To recheck the transgene insertion and to confirm the background, DNA was extracted for individual/master genotyping of different transgenic lines. Genomic DNA was extracted according to the protocol described by Edwards *et al*., (1991). For DNA extraction, a small proportion of *Arabidopsis* leaves were grinded into 1.5 mL microcentrifuge tubes containing 200 microliter of DNA extraction buffer (200 mM Tris-HCl, pH 7.5, 250 mM NaCl, 25 mM EDTA, 0.5% 20% SDS, in autoclaved ddH_2O water). Then, the samples were vortex at 13200rpm for 5 minutes. Afterwards, 150µl supernatant was collected in a fresh eppendorf tube, mixed with 150µl (1:1v/v) isopropanol and incubated at room temperature for 2 min. This step was followed by 5 min centrifugation at 13200rpm and after discarding supernatant, 500µl of ethanol was added to it. Again, supernatant was dumped after centrifugation and tubes were dried using speed vac for 15-20minutes or air dried overnight. Finally, the extracted DNA was resuspended in 50µl of ddH_2O and kept at 4 degree for further use. PCR was run ran using T100™ Thermal Cycler (Bio-Rad) to determine plant genotypes using gene-specific and mutant background specific primers using Columbia. Table 2 listed the primers used to identify background and gene specificity.

2.5 RNA extraction, cDNA synthesis and qPCR analysis

RNA extraction: Ten-days-old *Arabidopsis* transgenic seedlings grown on ½ MS plates, with or without 30µM estradiol, were sampled for RNA extraction. All the samples were immediately frozen in liquid nitrogen followed by −80°C storage. Total RNA was extracted from 6-8 independent T1 or T2 lines (with and without 30 µM Estradiol) with RNeasy Mini kit (Qiagen) according to manufacturer's instructions. First, tissues were grounded with prechilled blue pestle with liquid nitrogen, avoiding RNA degradation followed by addition of 450µl RLT buffer (premixed with beta-mercaptothion in 1:100 ratio). Eppendorf tubes were centrifuged quickly, and all the lysate was transferred to QIA shredder spin column, centrifuged at maximum speed for 2 min and 0.5 volume of 90% ethanol was mixed with supernatant. This solution was immediately transferred to the RNA binding column followed by addition of 350µl RW1 buffer and tubes were centrifuged at 10000rpm for 15 seconds. This step was followed by addition of 80µl DNAse1

(Qiagen) and incubation at room temperature for 15 min. After incubation, 350µl of RW1 buffer was added again and centrifuged at 10000rpm for 15 sec. Afterwards, 500µl of RPE buffer was added and tubes were centrifuged at 10000rpm for 15 sec followed by 2 min centrifugation at maximum speed. Finally, RNA was eluted in fresh 1.5ml microcentrifuge tube with RNAase free elution buffer and stored in -80 freezer.

cDNA synthesis: Total RNA (1.2 µg) except wheat RNA (100 ng) was used to synthesize single stranded cDNA by using iScript cDNA Synthesis Kit (Bio-Rad). Synthesized cDNA was used as reaction template after 1/10 dilution. The first-strand cDNA was generated by iScript cDNA Synthesis kit (Bio-Rad) using 1.2 µg of RNA, diluted 1:10 in double distilled water, and then used as a template for qPCR analysis. RT-qPCR were performed in CFX96 real time PCR detection system (Bio-Rad) using SsoAdvanced Universal SYBR Green Supermix (Bio-Rad). RT-qpCR was run under standard qPCR conditions by using a minimum of three technical and biological replicates. Data was normalized against *eIF4A* for genes in *Arabidopsis* and the Pfaffl method (Shaw *et al.*, 2012) was used to calculate the relative expression levels of the target genes. Gene specific primers used to detect transcripts are listed in Table 3.

2.6 Microscopy and quantitative analysis of stomatal phenotype

2.6.1 Confocal microscopy

Both *Arabidopsis* and *Brachypodium*'s epidermal cells phenotype were examined using a Nikon C2 laser scanning confocal microscope with a 40x bright objective lens. A very small section of leaf was excised and mounted in 5-10µl of propidium iodide (2mg/ml ddH_2O). A 561nm laser was used to excite PI fluorescence for imaging. To observe GFP signals, a standard GFP filter at 488nm excitation was used. For all imaging, an immersion oil of 1.49 refractive index was used for 40X lens. Emission wavelengths were filtered using a bandpass filter BP 525/50 for GFP and BP 561 for propidium iodide. All imaging processing was done with Fiji software and the images were false colored using Photoshop CS6 (Adobe).

2.6.2 Quantitative analysis of stomatal phenotype

Quantitative analysis of stomatal phenotypes was done using Toluidine Blue O (TBO) stained epidermal samples as described formerly (Guseman *et al*., 2010). To do so, abaxial cotyledons of 10-day-old *Arabidopsis* seedlings and base of first leaves of 6-8-day-old *Brachypodium* seedlings were fixed in 1 ml of fixing solution (9:1, ethanol: acetic acid respectively) for further imaging process. One day prior to imaging, fixed samples were subsequentially treated twice with 70%, 50%, 20% ethanol for a time period of 20 minutes each and finally, samples were stored in 1ml ddH_2O. Next day, samples were stained by adding 1ml of filtered, 0.5%(w/v) TBO stain in 1.5ml tubes having samples followed by 3-4min RT incubation. After removal of TBO stain, samples were immediately rinsed 4-5 time with ddH_2O. Samples were mounted in 15% glycerol and images were taken using Nikon Eclipse TiE inverted epifluorescence microscope equipped with a DsRi2 digital camera (Nikon). The number of stomata and other epidermal cells in each photograph were counted and converted into both the density and index for each cell type. The statistically significant differences in a panel of different genotypes were determined by either Tukey's HSD test after a one-way ANOVA ($P < 0.05$) or Student's t-test with P values of < 0.0001.

2.7 Chemical treatments

Transgenic *Arabidopsis* seedlings carrying estradiol-inducible constructs for *Arabidopsis* EPF peptides and their homologs from *Brachypodium* and wheat were germinated on ½ MS medium in the absence or presence of 30 μM estradiol (Sigma). The induction of *EPF* gene expression was confirmed by RT-qPCR analysis. The phenotypic consequence of induction was examined by observing the epidermal phenotype of cotyledons using a confocal microscope.

2.8 Production of peptides and bioassays

Expression and purification of *Brachypodium* EPF1 and EPF2 peptides were performed as described previously (Lee *et al*., 2012). Both, BdEPF1 and BdEPF2 peptides were expressed in *E. coli* overnight at 30°C and purified by a Ni column (His-Trap FF, GE Healthcare) after certain steps. Thereafter, these two recombinant peptides and chemically synthesized *Brachypodium* STOMAGEN-1 (Invitrogen) were dissolved in 20 mM Tris-HCl, pH 8.8, and 50 mM NaCl and refolded (Mini dialysis kit, MWCO:1,000, GE Healthcare) for 3 d at 4 °C using glutathione (reduced and oxidized forms; Sigma) and L-arginine ethyl ester dihydrochloride (Sigma). The peptides were further dialysed twice against 50 mM Tris-HCl, pH 8.0 for 1.5 days to remove glutathione. For bioassays, either buffer alone (mock: 50 mM Tris-HCl at pH 8.0) or *Brachypodium* MEPF peptides (2.5 μM) in buffer were applied to 1-day-old Bd21-3 seedlings in ½ MS liquid medium. After 5-7 days of further incubation, the epidermal phenotypes of *Brachypodium* leaves were examined with a Nikon C2 confocal microscopy and/or a Nikon Eclipse TiE microscope after TBO staining.

Table 1. List of plasmids constructed in this study and their description

Plasmid ID	Description	Insert	Vector	Bac R	Plant R
pJSL156	BdEPF1 in pKUT612 (pENTR-D-Keiko)	BdEPF1 cDNA	pKUT612	Kan	NA
pJSL151	proEst::BdEPF1	pJSL156	pER8	Spec/Strep	Hyg
pJSL157	BdEPF2 in pKUT612	BdEPF2 cDNA	pKUT612	Kan	NA
pJSL158	proEst::BdEPF2	pJSL157	pER8	Spec/Strep	Hyg
pJSL148	BdSTOMAGEN-1in pKUT612	BdSTOMAGEN-1 cDNA	pKUT612	Kan	NA
pJSL149	proEst::BdSTOMAGEN-1	pJSL148	pER8	Spec/Strep	Hyg
pJSL185	BdSTOMAGEN-2 in pKUT612	BdSTOMAGEN-2 cDNA	pKUT612	Kan	NA
pJSL187	proEst::BdSTOMAGEN-2	pJSL148	pER8	Spec/Strep	Hyg
pJSL171	TaEPF1 in pKUT612	TaEPF1 cDNA	pKUT612	Kan	NA
pJSL179	proEst::TaEPF1	pJSL171	pER8	Spec/Strep	Hyg
pJSL173	TaEPF2 in pKUT612	BdEPF2 cDNA	pKUT612	Kan	NA
pJSL180	proEst::TaEPF2	pJSL173	pER8	Spec/Strep	Hyg
pJSL177	TaSTOMAGEN-1in pKUT612	TaSTOMAGEN-1 cDNA	pKUT612	Kan	NA
pJSL181	proEst::TaSTOMAGEN-1	pJSL148	pER8	Spec/Strep	Hyg
pJSL188	proEst::TaSTOMAGEN-2	TsSTOMAGEN-2 cDNA	pER8	Spec/Strep	Hyg
pJSL193	EPF1 in pKUT612	EPF1 cDNA	pKUT612	Kan	NA
pRJ14	proEPF1::nucGFP (nls3xGFP)	pBK1(pEPF1 in pENTR 5'-TOPO), pKUT612	pAR132 (nls3xGFP in pGWB501 R4)	Spec/Strep	Hyg
pRJ21	proEPF1::EPF1	pBK1, pJSL193	pGWB501 R4	Spec	Hyg
pRJ6	proEPF1::BdEPF1	pBK1, pJSL156	pGWB501 R4	Spec	Hyg
pRJ13	proEPF1::BdEPF2	pBK1, pJSL157	pGWB501 R4	Spec	Hyg
pRJ9	proEPF1::TaEPF1	pBK1, pJSL171	pGWB501 R4	Spec	Hyg
pRJ18	proEPF1::TaEPF2	pBK1, pJSL173	pGWB501 R4	Spec	Hyg

Plasmid ID	**Description**	**Insert**	**Vector**	**Bac R**	**Plant R**
pJSL146	EPF2 promoter	*EPF2* promoter	pENTR/5'-TOPO	Kan	NA
pJSL194	EPF2 in pKUT612	EPF2 cDNA	pKUT612	Kan	NA
pRJ23	proEPF2::nucGFP	pJSL146, pKUT612	pAR132	Spec/Strep	Hyg
pRJ22	proEPF2::EPF2	pJSL146, pJSL194	pGWB501 R4	Spec	Hyg
pJSL175	proEPF2::BdEPF1	*EPF2* promoter	pJSL156	Kan	NA
pRJ17	proEPF2::BdEPF1	pJSL175	pGWB1	Kan/Hyg	Kan/Hyg
pRJ16	proEPF2::BdEPF2	pJSL146, pJSL157	pGWB501 R4	Spec	Hyg
pJSL190	proEPF2::TaEPF1	*EPF2* promoter	pJSL171	Kan	NA
pRJ20	proEPF2::TaEPF1	pJSL190	pGWB1	Kan/Hyg	Kan/Hyg
pRJ19	proEPF2::TaEPF2	pJSL146, pJSL173	pGWB501 R4	Spec	Hyg
pJSL198	pBAD::MBdEPF16xHIS	mature BdEPF1	pBADgIII	AMP	NA
pJSL199	pBAD::MBdEPF2-6xHIS	mature BdEPF2	pBADgIII	AMP	NA

Table 2. List of primers and their DNA sequence used for genotype analysis

Gene names	Primer names	Sequences (5' to 3')
TaEPF1	Ta2g526100 XhoIf	CACCCTCGAGATGATGATGAGGCATGGTCTTGT
	Ta2g526100 393 SpeI.rc	CGGACTAGTCTAGCTGGAGGGAACGGGGTAGCA
	Ta2g526100 390 SpeI.rc	CGGACTAGTGCTGGAGGGAACGGGGTAGCA
TaEPF2	Ta2g343000 XhoIf	CACCCTCGAGATGAGGAGGCCTGCTGGCGT
	Ta2g343000 423 SpeI.rc	CGGACTAGTCTAGAGGGCGGGGACGCGGAA
	Ta2g343000 420 SpeI.rc	CGGACTAGTGAGGGCGGGGACGCGGAAGAACCT
TaSTOMAGEN-1	Ta2g419900 SpeIf	CGGACTAGTATGGCCGGTGGTAGCCCCACAACT
	Ta2g419900 369 SpeI.rc	CGGACTAGTTCACCTGTGGCAGACACACTTGTA
	Ta2g419900 366 SpeI.rc	CGGACTAGTCCTGTGGCAGACACACTTGTAATG
TaSTOMAGEN-2	Ta2g255900 SpeIf	CGGACTAGTATGACTGGAGTGGGAAGAAACAGGC T
	Ta2g255900 354 SpeI.rc	CGGACTAGTGACATGGCAGAAACATCTGTAGTGGT
	Ta2g255900 357 SpeI.rc	GCCACTAGTCTAGACATGGCAGAAACATCTGTAGT GGTAGG
BdEPF1	Bd5g12220 XhoIf (GW)	CACCCTCGAGATGAGGAGGTTTACTCGCGTT
	Bd5g12220 429 SpeI.rc	CGGACTAGTTACGGTGGGAGAGCTGCTGACGA
	Bd5g12220 426 SpeI.rc	CGGACTAGTCGGTGGGAGAGCTGCTGACGAGA
BdEPF2	Bd5g23357 XhoIf (GW)	CACCCTCGAGATGGCCGCTTGCTGCTGCTGCT
	Bd5g23357 573 SpeI.rc	CGGACTAGTTAGCTGGAGGGCACGGGGTAGCA
	Bd5g23357 570 SpeI.rc	CGGACTAGTGCTGGAGGGCACGGGGTAGCA
BdSTOMAGEN-1	Bd2g58540 XhoIf (GW)	CACCCTCGAGATGGCCAGTGGTTGCCCCACAA
	Bd2g58540 369 SpeI.rc	CGGACTAGTCACCTGTGGCAGACACACTTGTAAT
	Bd2g58540 366 SpeI.rc	CGGACTAGTCCTGTGGCAGACACACTTGTAAT
BdSTOMAGEN-2	Bd3g40846 XhoIf (GW)	CACCCTCGAGATGCGGGCGTTATGCTACGTGT
	Bd3g40846 369 SpeI.rc	CGGACTAGTCTAGGCATGGCAGAAGCACCTGT
	Bd3g40846 366 SpeI.rc	CGGACTAGTGGCATGGCAGAAGCACCTGT

Table 3. List of qRT-PCR primers and their DNA sequence used

Gene names	Primer names	Sequences (5'-3')
TaEPF1	Ta2g526100 113f	CCGATGATGCTGATGCAAGA
	Ta2g526100 241.rc	CGTCCCGTACACCTCCT
TaEPF2	Ta2g343000 94f	AGAACCACACCAAGTTCAGGC
	Ta2g343000 220.rc	CTCCCGCTTCTGCTGATTTC
TaSTOMAGEN-1	Ta2g419900 40f	CTCCTCTTCTTCCTCCTCTCTTC
	Ta2g419900 150.rc	GGTAATCCCTGGTGAGCATATTC
TaSTOMAGEN-2	Ta2g255900 24f	GCTGCTGTTGATCTGCTATCTC
	Ta2g255900 140.rc	CTAAGCCCTCATGTTCTGTCTCC
EIF4A	EIF4A 962f	AGCCAGTGAGAATCTTGGTGAAGC
	EIF4A 1543.rc	CTAGTACGGCAGAGCAAACACAGC
BdEPF1	Bd5g12220 85f	GTCAGAGCAACACCAAGTG
	Bd5g12220 168.rc	TGCAGACTGTGTCATCTTAC
BdEPF2	Bd5g23357 297f	CGTCATGGTCAGCTTCAAGT
	Bd5g23357 375.rc	GTAGCACTTGCCCTTGCACAT
BdSTOMAGEN-1	Bd2g58540 95f	GTTACCATGGCAGCACCTCA
	Bd2g58540 223.rc	TCCTTGCATACTTGGGCAGT
BdSTOMAGEN-2	Bd3g40846 8f	CGTTATGCTACGTGTTCCTC
	Bd3g40846 86.rc	TGAGCAGCTGCTAGAACGAC

3. Results

3.1. Identification of EPF family of signaling peptides in grasses

Our goal was to identify the possible homologs of EPF/EPFL-like genes in cereal grasses as model dicot plant *Arabidopsis* known to possess 11 EPFs in total. To find out EPF homologs in cereal crops, numerous accessible databases of genomic sequence were searched by our collaborator Dr. Patrick Gulick lab members. It was followed by initial in-silico phylogenetic analysis of EPF homologs in various grass species.

As shown in Figure. 5, phylogenetic analysis revealed that there are 12-15 genes encoding putative EPFs in each of the grass species examined. Each EPF gene possesses six or eight conserved cysteines in the predicted mature EPF (MEPF) domain at its C-terminal ends, which are critical for the biological activity of secreted cysteine-rich peptides, including *Arabidopsis* EPFs. Among 11 *Arabidopsis* EPF family members, stomatal EPF peptides AtEPF1, AtEPF2, and AtSTOMAGEN are the most well-characterized EPFs, and we found two *EPF1/EPF2*-like genes that have homology to the C-terminus of *AtEPF1* and *AtEPF2*, the closest *Arabidopsis* EPF family members, and two *STOMAGEN*-like genes in each of the cereal crop and the grass model organism, *Brachypodium distachyon*. Whereas, in model dicot plant *Arabidopsis*, only one copy of *STOMAGEN* exists. For further experiments, we decided to proceed with stomatal EPF homologs in *Brachypodium*, a model monocot plant and Wheat, economically one of the most important crops (**Figure 5).**

Altogether, these observations provide the evidence of presence and conservation of possible functions of secreted EPF peptides in controlling various developmental processes in both dicots and monocots, although their specific roles in grasses remain unclear.

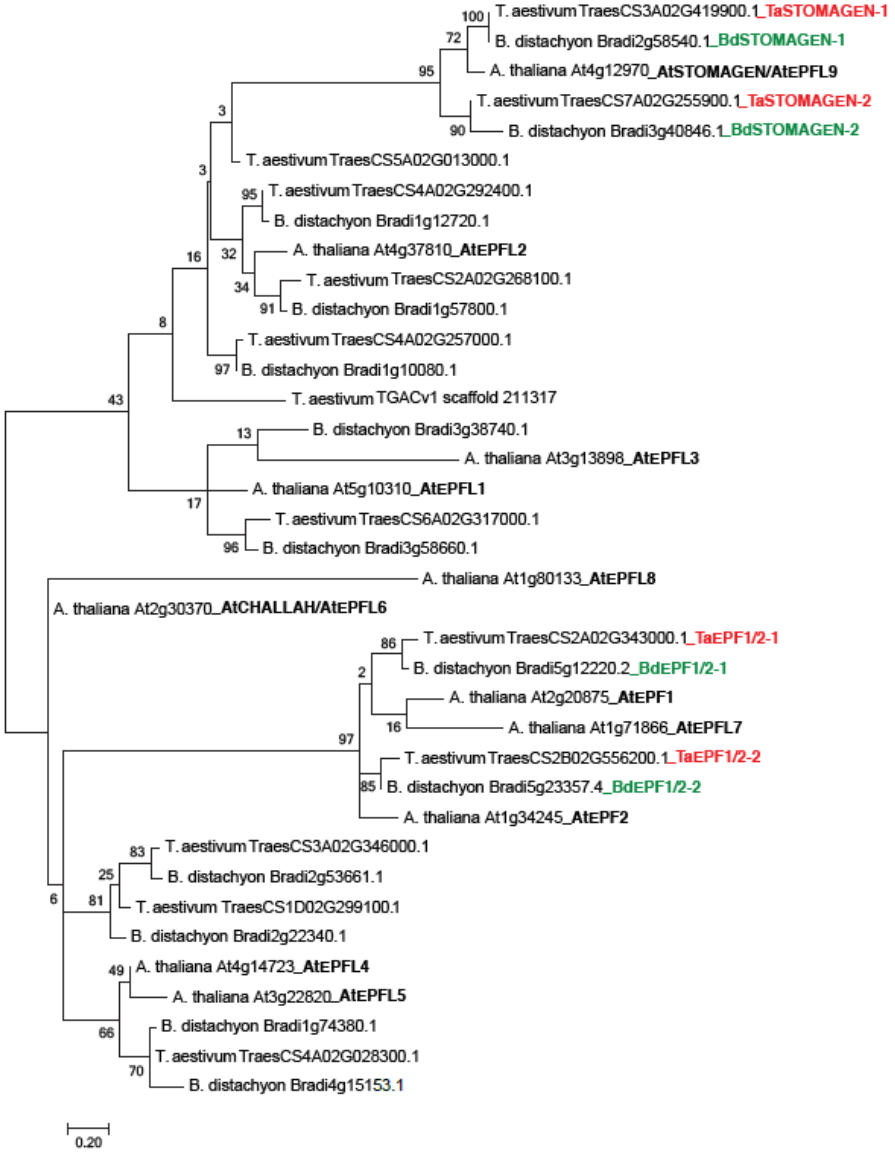

Figure 5. Identification of different EPF homologs in grasses

This phylogenetic tree was constructed by using a Jones Taylor Thornton (JTT) model. A total of 87 amino acid sequence were analysed. All the analysis was done by using MEGA software (version 7.0) (Kumar *et al.*, 2016). All 3 stomatal EPF homologous genes of *Brachypodium distachyon* and *Triticum aestivum* are highlighted in green and red colour respectively.

3.2 Characterization of different monocotyledonous stomatal EPFs using *Arabidopsis* system

Among 11 *Arabidopsis* EPF family peptides, stomatal EPFs are the well- characterized EPF family members to this date, and the biological roles of some other EPFs remain unknown. To gain insight into the functional importance and conservation of grass EPF homologs, we conducted further analyses using a subset of grass EPFs that have sequence similarity to *Arabidopsis* stomatal EPF peptides; EPF1, EPF2, STOMAGEN in both *Brachypodium distachyon* and *Triticum aestivum* (**Figure 5, green & red highlighted)**.

3.2.1 *STOMAGEN* function is conserved in dicots and grasses

To determine the function of grass homologs of AtSTOMAGEN, we first generated transgenic *Arabidopsis* plants overexpressing each of two *STOMAGEN*-like genes in *Brachypodium*, (*BdSTOMAGEN-1* and *BdSTOMAGEN-2*), and wheat (*TaSTOMAGEN-1* and *TaSTOMAGEN-2*) using an estradiol-induction system. This was followed by sowing of *Arabidopsis* seeds carrying inducible *Bd/TaSTOMAGEN-1* and *Bd/TaSTOMAGEN-2* overexpressed transgenes on 1/2 MS media plates supplemented with and without estradiol. At 10 dpg, more than 40 T1 or T2 generation seedlings (in presence and absence of inducer) were screened to check epidermal phenotype of both *Bd/TaSTOMAGEN-1OE* and *Bd/TaSTOMAGEN-2OE* lines. In parallel, we also sowed and imaged *AtSTOMAGEN* overexpression lines as a reference to compare phenotype of grass *STOMAGEN* homologous gene.

Ectopic expression of grass homologs of *AtSTOMAGEN* resulted into a phenotype of increased stomatal density and clusters in presence of estradiol **(Figure 6 E, F, K, L)**. These transgenes showed a phenotype like wild type Col when estradiol was absent in the media plates **(Figure 6 B, C, H, I)**. Induced *AtSTOMAGEN* also showed increased production and clustering of stomata in *Arabidopsis* **(Figure 6 D)**. As expected, in absence of estradiol, *AtSTOMAGEN* phenotype appeared like wild type **(Figure 6 A)**. We also used *Arabidopsis* wild type, Columbia, as another control and treated it with same concentration of estradiol. As a result, there were no changes in 10dpg epidermal phenotype irrespective of presence and absence of inducer in *Arabidopsis* wild type seedlings **(Figure 6 G, J)**. It clearly showed that all the phenotypes observed were due to

presence of *Brachypodium* and wheat EPF transgenes not because of only estradiol induction system.

Furthermore, we reconfirmed above mentioned results by performing quantitative analysis of epidermal cells. To do so, TBO (Toluidine Blue O) analysis were performed by using 10dpg seedlings in which stomatal index was quantified as the percentage of total stomatal number to the total number of stomatal and non-stomatal cells. Similar to the effects of an induced *AtSTOMAGEN* overexpression, we observed an abrupt increase in stomatal index in transgenic *Arabidopsis* plants carrying induced grass *STOMAGEN* homologs as compare to uninduced lines **(Figure 6 M)**.

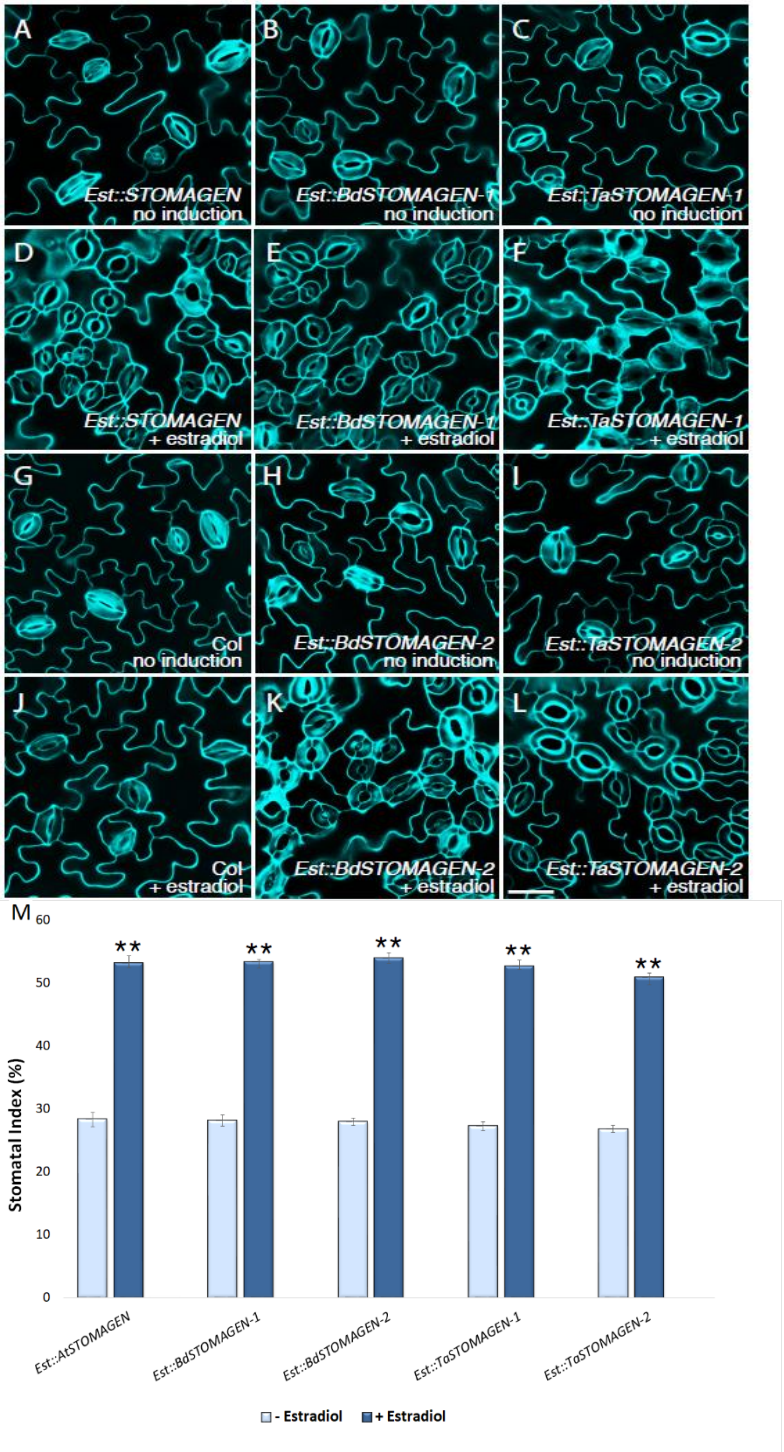
A
Est::STOMAGEN
no induction
B
Est::BdSTOMAGEN-1
no induction
C
Est::TaSTOMAGEN-1
no induction
D
Est::STOMAGEN
+ estradiol
E
Est::BdSTOMAGEN-1
+ estradiol
F
Est::TaSTOMAGEN-1
+ estradiol
G
Col
no induction
H
Est::BdSTOMAGEN-2
no induction
I
Est::TaSTOMAGEN-2
no induction
J
Col
+ estradiol
K
Est::BdSTOMAGEN-2
+ estradiol
L
Est::TaSTOMAGEN-2
+ estradiol
M
Stomatal Index (%)
60
50
40
30
20
10
0
**
Est::AtSTOMAGEN
Est::BdSTOMAGEN-1
Est::BdSTOMAGEN-2
Est::TaSTOMAGEN-1
Est::TaSTOMAGEN-2
- Estradiol
+ Estradiol

Figure 6. *STOMAGEN* positively regulates stomatal development in grasses

(A-L) Representative confocal images of 10-days-old abaxial cotyledons of the following genotypes: uninduced *Est::STOMAGEN* (A), uninduced *Est::BdSTOMAGEN-1* (B), uninduced *Est::TaSTOMAGEN-1* (C), induced *Est::STOMAGEN* (D), induced *Est::BdSTOMAGEN-1* (E), induced *Est::TaSTOMAGEN-1* (F), uninduced Col (G), uninduced *Est::BdSTOMAGEN-2* (H), uninduced *Est::TaSTOMAGEN-2* (I), induced Col (J), induced *Est::BdSTOMAGEN-2* (K), induced *Est::TaSTOMAGEN-2* (L). Sample size screened to find each STOMAGEN homolog phenotype n=40-45. Cells were outlined by propidium iodide staining and images were taken under the same magnification. Scale bar = 30 μm.

(M) Graph shows quantitative analysis of 10-days-old abaxial cotyledon epidermis. Stomatal index (SI) of uninduced and induced *Arabidopsis*, *Brachypodium* and Wheat *STOMAGEN-1* & *STOMAGEN-2* homologs expressed as the percentage of the number of stomata to the total number of epidermal cells. ($P < 0.05$, Tukey's HSD test after one-way ANOVA). $n = 8$-9 for each genotype. Asterisks indicate significant differences compared within genotypes in presence and absence of estradiol inducer. The experiments were repeated three times with similar results. Bars, means. Error bars, SE.

To support above mentioned phenotypic and statistical analysis, induction of grass *STOMAGEN* homologs were confirmed by checking expression of 12-15 T1 or T2 individual transgenic lines simultaneously. To do so, Reverse Transcription-PCR (RT-PCR) was performed for 12-15 T1 or T2 individual transgenic lines.

Afterwards, qPCR was performed by using selected 6-8 positive lines which were selected on basis of RT-PCR results. qPCR results showed that the mRNA expression level of both induced *BdSTOMAGEN-1* (line number 1, 3 and 14) and *BdSTOMAGEN-2* (line number 1, 2 and 4) were significantly higher than their respective controls (in absence of estradiol) **(Figure 7 A, B)**.

Expression levels of wheat *STOMAGEN-1/2* homologs were also found to be upregulated upon induction with estradiol inducer. In *TaSTOMAGEN-1* and *TaSTOMAGEN-2* homologs, induced line showed higher transcript level were line number 3, 4, 12 and 1, 2, 4 respectively **(Figure 8 C, D)**. Hence, it can be assumed that function of grasses' *STOMAGEN* is conserved as a positive stomatal regulator in both dicots and monocots.

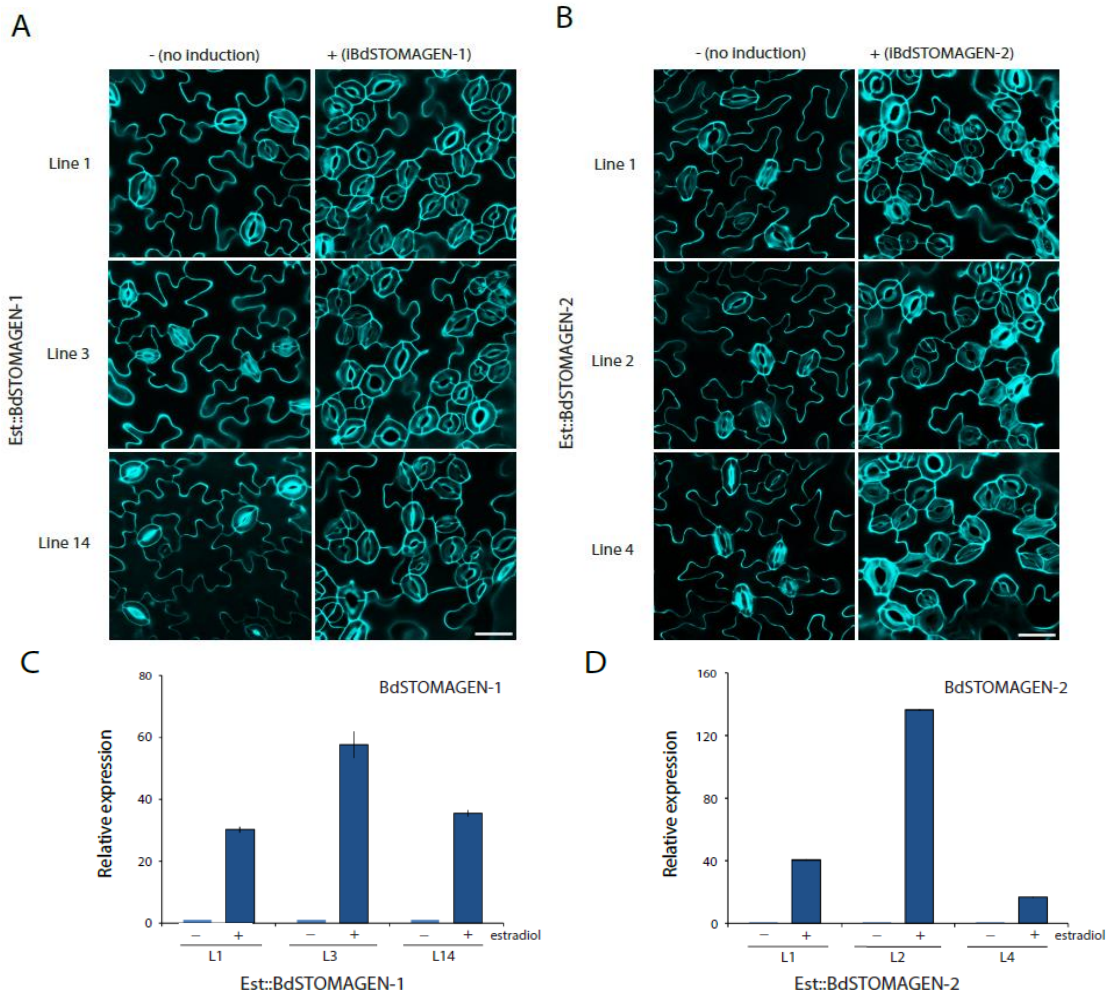

Figure 7. Epidermis phenotype of induced overexpression of *Brachypodium STOMAGEN* homologs in multiple independent *Arabidopsis* transgenic lines

(A-B) Representative confocal images of abaxial cotyledon epidermis from 3 independent *Arabidopsis* transgenic lines harboring an estradiol-inducible overexpression construct for BdSTOMAGEN-1 (A) and BdSTOMAGEN-2 (B). Left panels, no induction (control); right panels, estradiol induction; each row shows representative images from individual lines. Cells were outlined by propidium iodide staining and images were taken under the same magnification. Scale bar = 30 µm. (C-D) qPCR analyses of *BdSTOMAGEN-1* (C) and *BdSTOMAGEN-2* (D) transgenes in three independent *Arabidopsis* transgenic plants carrying estradiol-inducible overexpression constructs for *Brachypodium* STOMAGEN homologs. *eIF4A* was used as an internal control and the data for each uninduced transgenic line were set to 1. Error bars; means with SE (n = 3).

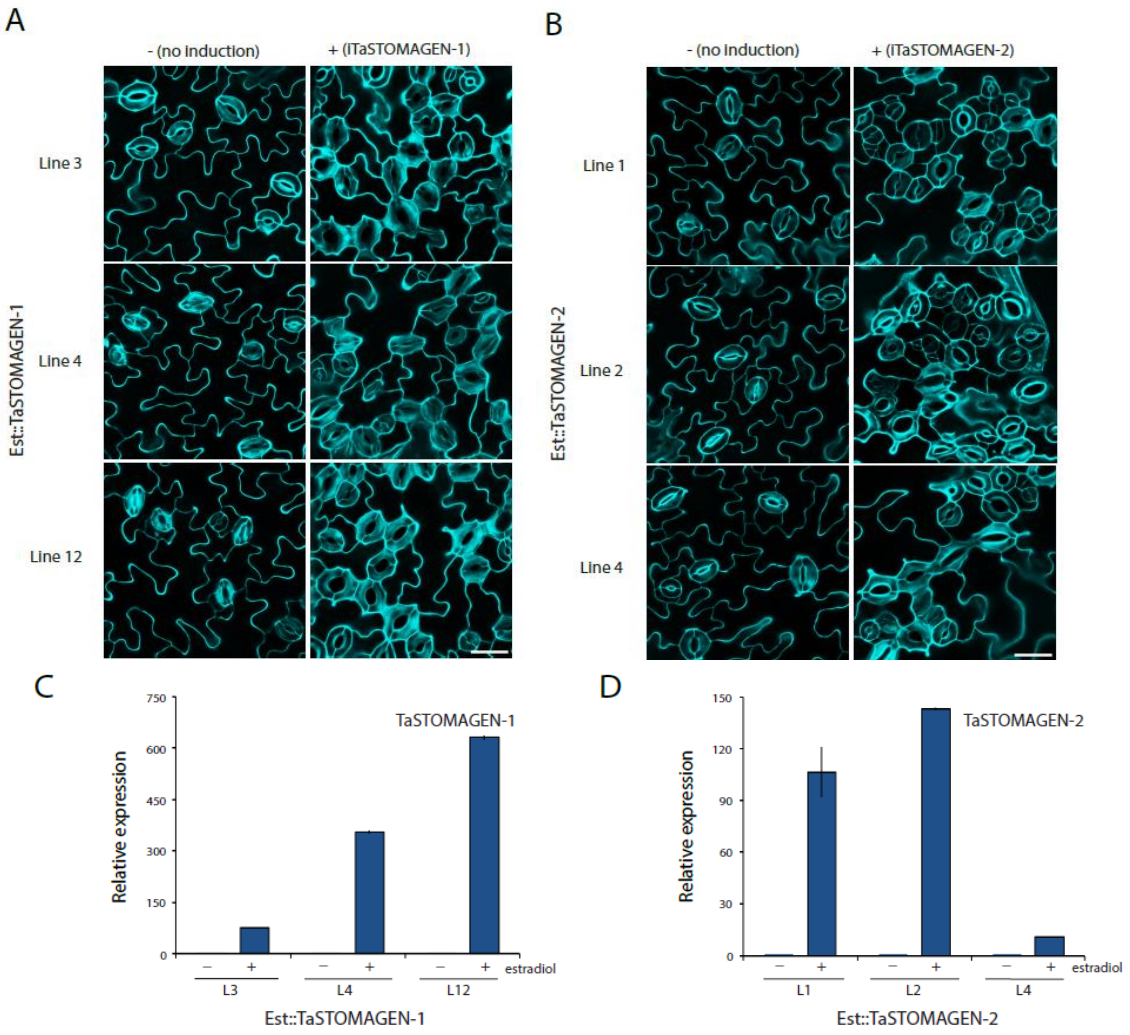

Figure 8. Epidermis phenotype of induced overexpression of wheat STOMAGEN homologs in multiple independent *Arabidopsis* transgenic lines

(A-B) Representative confocal images of abaxial cotyledon epidermis from 3 independent *Arabidopsis* transgenic lines harboring an estradiol-inducible overexpression construct for TaSTOMAGEN-1 (A) and TaSTOMAGEN-2 (B). Left panels, no induction (control); right panels, estradiol induction; each row shows representative images from individual lines. Cells were outlined by propidium iodide staining and images were taken under the same magnification. Scale bar = 30 µm. (C-D) qPCR analyses of *TaSTOMAGEN-1* (C) and *TaSTOMAGEN-2* (D) transgenes in three independent *Arabidopsis* transgenic plants carrying estradiol-inducible overexpression constructs for wheat STOMAGEN homologs. *eIF4A* was used as an internal control and the data for each uninduced transgenic line were set to 1. Error bars; means with SE (n = 3).

3.2.2 Overexpression of grass *EPF1/EPF2*-like genes decreases stomatal density without any arrested meristemoid cells in *Arabidopsis*

Next, to determine the effect of ectopic expression of grass homolog of EPF1 and EPF2, two negative stomatal signals identified in *Arabidopsis*, we generated transgenic plants overexpressing individual *EPF1* and *EPF2*-like genes in *Brachypodium*, (*BdEPF1/2*), and wheat (*TaEPF1/2*) using an estradiol-induction system. We also used estradiol inducible *AtEPF1OE* and *AtEPF2OE* lines as controls to compare the phenotype of overexpressed *Bd/TaEPF1* and *Bd/TaEPF2* homologs in *Arabidopsis*.

Due to their highest sequence similarity to two *Arabidopsis* EPF peptides, we speculated that each of two *EPF1/EPF2*-like genes found in wheat and *Brachypodium* would behave like their corresponding peptides in *Arabidopsis*, AtEPF1 and AtEPF2, respectively. As previously reported, ectopic expression of one of two negative stomatal peptides, *iAtEPF2*, led to the epidermis devoid of stomata, which resulted in dramatically decreased stomatal density **(Figure 9 D)**.

As anticipated, *EPF2*-like genes in both *Brachypodium* and wheat, *iBdEPF2* and *iTaEPF2*, also led to the epidermis with only pavement cells in each of >40 T1 or T2 transgenic lines examined for each construct **(Figure 9 E, F)**. Whereas in absence of estradiol, uninduced *AtEPF2OE* and *Bd/TaEPF2OE* did not acquire any phenotype, hence, looked like *Arabidopsis* wild type phenotype **(Figure 9 A, B, C)**. Meanwhile, to quantify the expression level of *iBd/TaEPF2* homologs, qPCR was also performed for 6-8 T1 or T2 transgenic lines carrying these genes . We found that upon treatment with estradiol, seedlings carrying *BdEPF2OE* (line 10, 11, 12) and *TaEPF2OE* (line 4, 5, 19) transgenes showed higher transcriptional expression level as compare to seedlings grown without estradiol inducer **(Figure 10 A, B, C, D)**.

Along with phenotypic and qPCR analysis, quantitative analysis of epidermal phenotype was also performed by counting number of stomatal and non-stomatal cells in both induced and induced *Bd/TaEPF2OE* and *AtEPF2OE* (control) lines. This was performed by staining 10dpg *Arabidopsis's* cotyledons with Toluidine Blue O (TBO) stain followed by quantification of leaf epidermal cells. As shown in Figure 9, we observed that stomatal index (number of stomata per total number of epidermal cells) was significantly reduced ($P < 0.05$, ANOVA) in *iBd/TaEPF2OE*

but remains comparable to wild type Columbia in uninduced *Bd/TaEPF2OE* constructs **(Figure 9 G)**. This data was consistent with our previous phenotypic analysis where both *Bd/TaEPF2* homologs showed an epidermis devoid of stomata and any stomatal lineage cells.

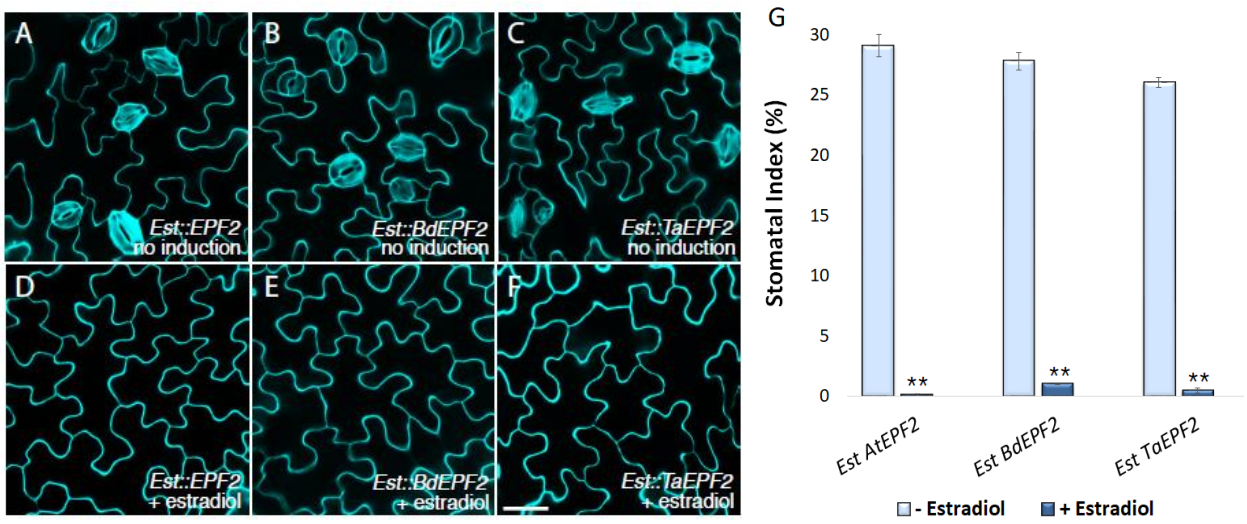

Figure 9. Both *Brachypodium* and wheat *EPF2* (*Bd/TaEPF2*) negatively regulates stomatal development in *Arabidopsis*

(A-F) Representative confocal images of 10-days-old abaxial cotyledons of the following genotypes: uninduced *Est::EPF2* (A), uninduced *Est::BdEPF2* (B), uninduced *Est::TaEPF2* (C), induced *Est::EPF2* (D), induced *Est::BdEPF2* (E), induced *Est::TaEPF2* (F). Sample size screened to find each genotype's phenotype n=40-45. Cells were outlined by propidium iodide staining and images were taken under the same magnification. Scale bar = 30 µm.

(G) Graph shows quantitative analysis of 10-days-old abaxial cotyledon epidermis. Stomatal index (SI) of uninduced and induced *Arabidopsis*, *Brachypodium* and Wheat *EPF2* homologs expressed as the percentage of the number of stomata to the total number of epidermal cells. ($P < 0.05$, Tukey's HSD test after one-way ANOVA). n = 14-15 for each genotype. Asterisks indicate significant differences within genotypes in presence and absence of estradiol inducer. The experiments were repeated three times with similar results. Bars, means. Error bars, SE.

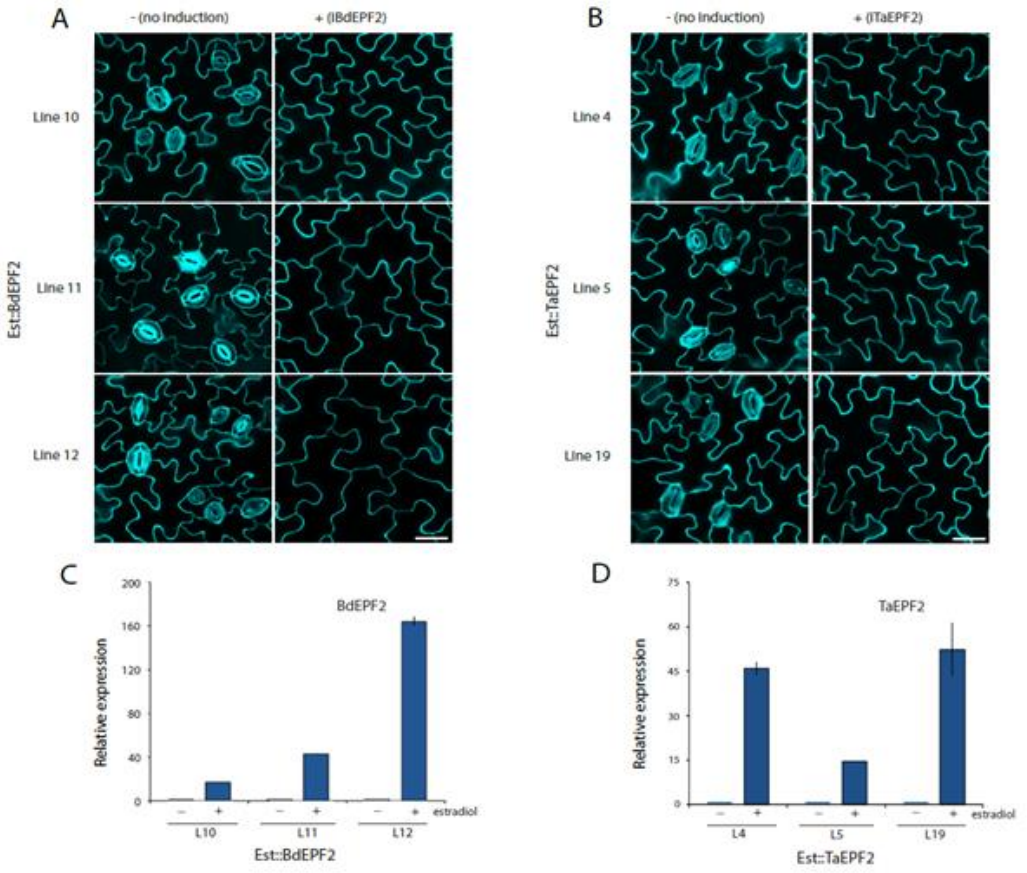

Figure 10. Epidermis phenotype of induced overexpression of *Brachypodium* and wheat EPF2 homolog in multiple independent *Arabidopsis* transgenic lines

(A) Representative confocal images of abaxial cotyledon epidermis from 3 independent *Arabidopsis* transgenic lines harboring an estradiol-inducible overexpression construct for BdEPF2 **(A)** and TaEPF2 **(B)**. Left panels, no induction (control); right panels, estradiol induction; each row shows representative images from individual lines. Cells were outlined by propidium iodide staining and images were taken under the same magnification. Scale bar = 30 µm. qPCR analyses of *BdEPF2* (**C**) and *TaEPF2* (**D)** transgenes in three independent *Arabidopsis* transgenic plants carrying estradiol-inducible overexpression constructs for *Brachypodium* and wheat EPF2 homolog. *eIF4A* was used as an internal control and the data for each uninduced transgenic line were set to 1. Error bars; means with SE (n = 3).

Next, we examined overexpression lines of *Brachypodium* and wheat EPF1 homolog (*Bd/TaEPF1*) and used *Arabidopsis EPF1* as a control. Consistent with its distinct functions during stomatal development in *Arabidopsis*, overexpression of *AtEPF1* led to an epidermis with arrested stomatal precursors, which resulted in significantly increased non-stomatal cell density. In addition, being a negative stomatal peptide, *iAtEPF1* led to the epidermis devoid of stomata **(Figure 11 D)**.

However, we found that *EPF1*-like genes in *Brachypodium*, i*BdEPF1* led to an epidermis devoid of all stomatal lineage cells in each of >40 T1 or T2 transgenic lines examined for each transgene **(Figure 11 E)**. Likewise, wheat *iTAEPF1* overexpression resulted in inhibition of the entry of stomatal lineage, a phenotype identical to induced *Arabidopsis EPF2* overexpression **(Figure 11 F).** Whereas uninduced *Bd/TaEPF1OE* lines had shown a phenotype resembled to *Arabidopsis* wild type phenotype **(Figure 11 A, B, C)**. Both induced *Bd/TaEPF1* transgenic lines were also used to quantify mRNA expression level. A significant increase in EPF1 transcripts accumulation in presence of estradiol were observed in both *BdEPF1* (line number 2, 7, 13) and *TaEPF1* (line number 1, 2, 3). Whereas their respective uninduced lines did not show any expression upregulation in monocot EPF1 homologs **(Figure 12 A, B, C, D)**.

Quantitative analysis of epidermal cells also confirmed the same results as mentioned above. Our statistical data showed that upon overexpression of both *Bd/TaEPF1* genes, stomatal index (percentage of total stomatal number to the total number of epidermal cells) decreased dramatically **(Figure 11 G)**. Due to presence of arrested stomatal precursors, overexpression of *AtEPF1* resulted into a significant increase in non-stomatal cell density (number of non-stomatal epidermal cells per mm^2) but did not change in any of grass EPF1 homologs **(Figure 11 H)**.

These observations demonstrate that all examined grass homologs of AtEPF1 and AtEPF2, when expressed in *Arabidopsis*, have *Arabidopsis* EPF2-like biological activity, rather than AtEPF1-like activity, which restricts entry asymmetric divisions during stomatal development in *Arabidopsis.*

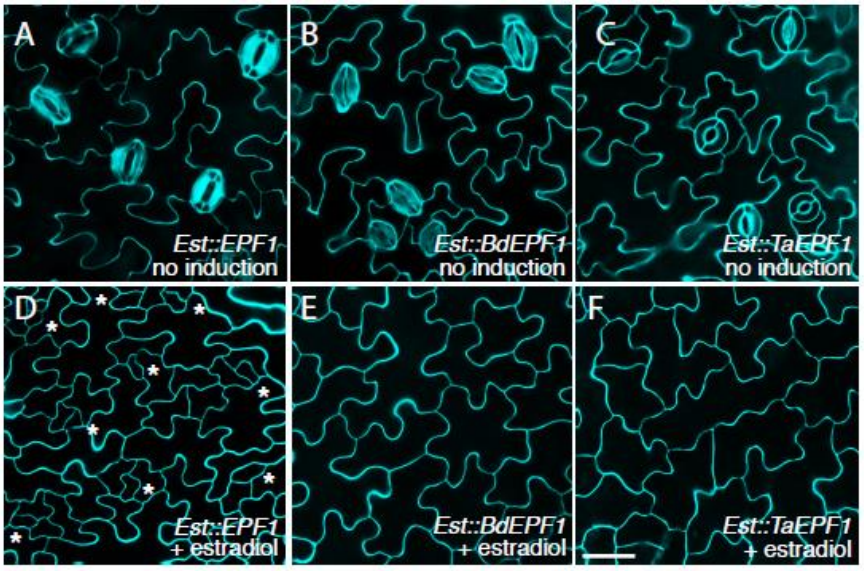
A
Est::EPF1
no induction
B
Est::BdEPF1
no induction
C
Est::TaEPF1
no induction
D
Est::EPF1
+ estradiol
E
Est::BdEPF1
+ estradiol
F
Est::TaEPF1
+ estradiol

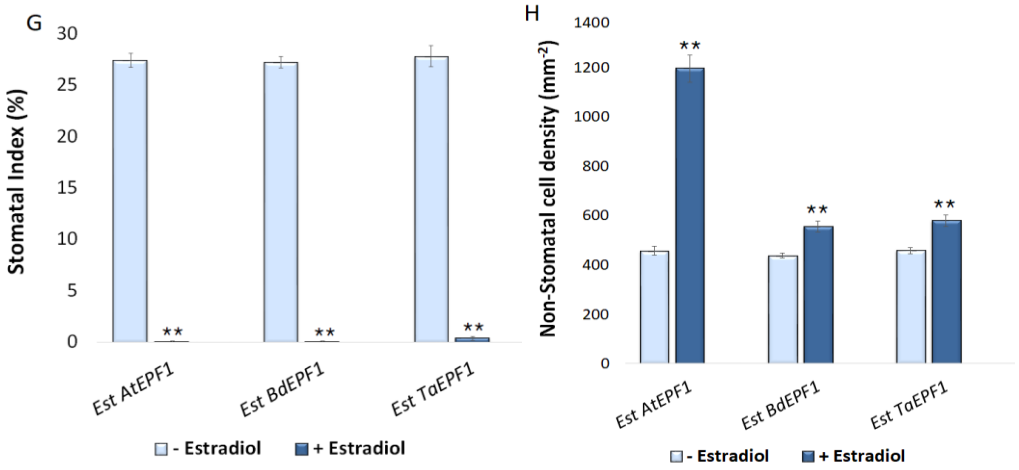
G
Stomatal Index (%)
30
25
20
15
10
5
0
**
Est AtEPF1
Est BdEPF1
Est TaEPF1
- Estradiol
+ Estradiol
H
Non-Stomatal cell density (mm-2)
1400
1200
1000
800
600
400
200
0
**
Est AtEPF1
Est BdEPF1
Est TaEPF1
- Estradiol
+ Estradiol

Figure 11. Effects of overexpression of *Bd/TaEPF1* on epidermal development of *Arabidopsis* seedlings

(A-F) Representative confocal images of 10-days-old abaxial cotyledons of the following genotypes: uninduced *Est::EPF1* (A), uninduced *Est::BdEPF1* (B), uninduced *Est::TaEPF1* (C), induced *Est::EPF1* (D), induced *Est::BdEPF1* (E), induced *Est::TaEPF1* (F). Sample size screened to find each genotype's phenotype n=45-50. Cells were outlined by propidium iodide staining and images were taken under the same magnification. Scale bar = 30 μm.

(G) Quantitative analysis of 10-days-old abaxial cotyledon epidermis. Stomatal index (SI) of uninduced and induced wild type, *Brachypodium* and wheat *EPF1* homologous is expressed as the percentage of the number of stomata to the total number of epidermal cells. Asterisks above the column indicate significant difference compared with data from wild type plants. ($P < 0.05$, Tukey's HSD test after one-way ANOVA). n = 8-9 for each genotype. The experiments were repeated three times with similar results. Bars, means. Error bars, SE.

(H) Non- Stomatal cell density (NSD) of uninduced and induced *Brachypodium* and wheat *EPF1* homologouss expressed as the number of non-stomatal cells to the total number of epidermal cells. Asterisks above the column indicate significant difference compared with data from wild type plants. ($P < 0.05$, Tukey's HSD test after one-way ANOVA). n = 8-9 for each genotype. The experiments were repeated three times with similar results. Bars, means. Error bars, SE.

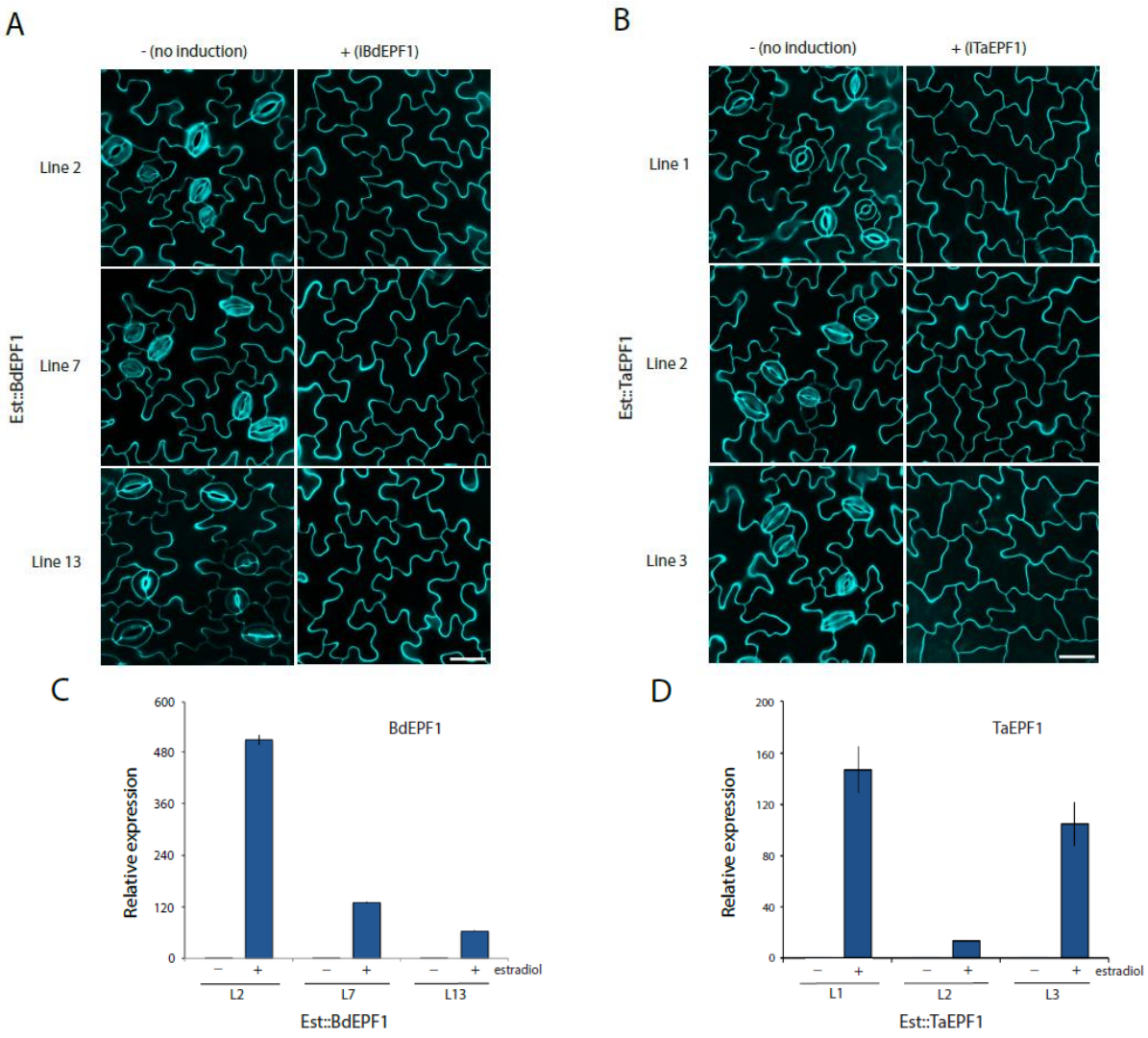

Figure 12. Epidermis phenotype of induced overexpression of *Brachypodium* and wheat EPF1 homolog in multiple independent *Arabidopsis* transgenic lines

(A) Representative confocal images of abaxial cotyledon epidermis from 3 independent *Arabidopsis* transgenic lines harboring an estradiol-inducible overexpression construct for BdEPF1 **(A)** and TaEPF1 **(B)**. Left panels, no induction (control); right panels, estradiol induction; each row shows representative images from individual lines. Cells were stained by propidium iodide and images were taken under the same magnification. Scale bar = 30 µm. qPCR analyses of *BdEPF1* **(C)** and *TaEPF1* **(D)** transgenes in three independent *Arabidopsis* transgenic plants carrying estradiol-inducible overexpression constructs for *Brachypodium* and wheat EPF1 homolog. *eIF4A* was used as an internal control and data for each uninduced transgenic line were set to 1. Error bars; means with SE (n = 3).

3.3 Cross-species complementation assay of *Bd/TaEPF1* and *Bd/TaEPF2* homologs by using respective *Arabidopsis's EPFs* Promoter

Because none of the grass *EPF1/2* homologs we tested, behaved like AtEPF1 signaling peptide in *Arabidopsis*, and since our findings differed from recently published data for certain monocot species (Caine *et al*., 2018; Hepworth *et al*., 2017; Dunn and Hunt, 2019), we further investigated the behavior of wheat and *Brachypodium EPF1/EPF2*-like genes in the regulation of epidermal development by analyzing the cross-species complementation studies.

Here, we solicited if 2 monocots' homologous genes, *EPF1* and *EPF2*, could rescue loss of function *epf1* and *epf2* mutant phenotype in *Arabidopsis* system. For this purpose, we performed cross species complementation assay and expressed each of the grass *EPF1/2* homolog in *epf1* and *epf2* mutants under the control of respective *Arabidopsis* promoters to drive their expression into distinct stages of stomatal lineage where *AtEPF1* and *AtEPF2* normally expressed in *Arabidopsis.*

3.3.1 Both *AtEPF1* and *AtEPF2* promotors had specific expression pattern restricted to various stomata lineage cells

Before performing cross species complementation assay by using *Arabidopsis EPF1* and *EPF2* promotors, we first confirmed the expression pattern of these promotors in specific stomatal precursor cells. To do so, these promotors were fused with nls:3XGFP and GFP reporter activity driven by these promotors were checked in the corresponding stomatal precursors in epidermis. Expression pattern of GFP showed that these two promotors expressed in early cell stages of stomatal formation. *AtEPF1* expression was observed in late meristemoids, guard mother cell and young guard cells (**Figure 13 A)** (Hara *et al*., 2007). Whereas *AtEPF2* expression was restricted only to early developmental cell stages i.e. meristemoid mother cells (MMCs) and early meristemoids (**Figure 13 B)** (Hara *et al*., 2009). Therefore, all the transgenes fused to these promotors should form their protein product correctly after initiation of transcription by these *Arabidopsis* promotors.

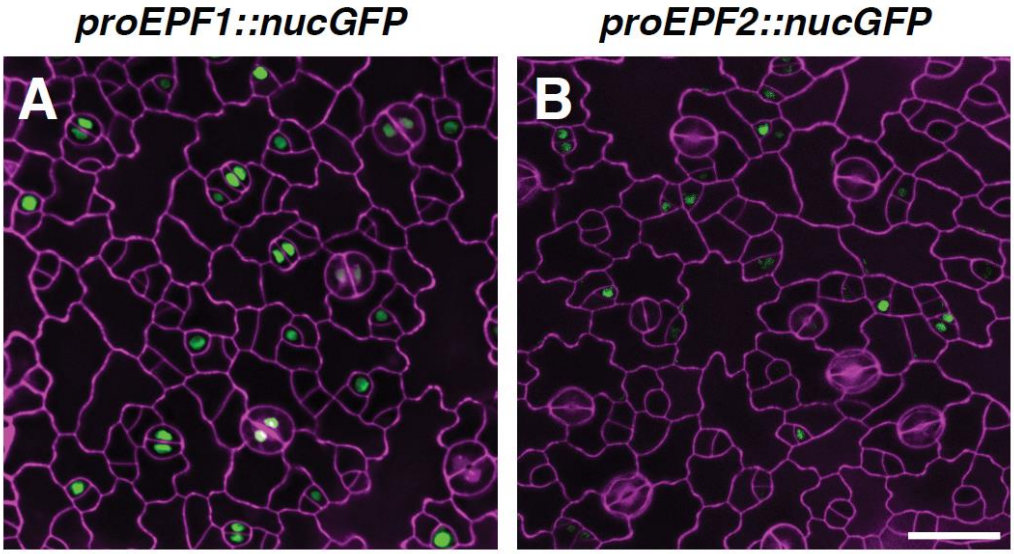

Figure 13. *AtEPF1* and *AtEPF2* promotors are active in stomatal lineage cells

Expression of *EPF1 promotor::nucGFP* (A) and *EPF2 promotor::nucGFP* (B) in abaxial true leaves of *Arabidopsis* to monitor GFP expression in stomatal lineage cells. To highlight the outline of cells, true leaves were stained with Propidium Iodide (PI, red colour). Fiji software was used for false colouring of cell outlines (Purple colour). Scale bar = 30 µm.

3.3.1. Grass *EPF1/EPF2* homolog failed to complement the epidermal phenotypes of *Arabidopsis epf1* mutants

We further investigated cross-complementation constructs of *Brachypodium* and *Triticum EPF1/2*; *AtEPF1pro::BdEPF1/2* and At*EPF1pro::TaEPF1/2*, in *Arabidopsis epf1* mutant background. The *epf1* loss-of-function mutant exhibited mild stomatal clustering phenotype because of defects in spacing divisions (Hara *et al*., 2007). As shown in Figure 14, none of the genotypes expressing grass EPF1 homolog (*AtEPF1pro::BdEPF1* and At*EPF1pro::TaEPF1*) were able to suppress *epf1*'s paired stomata phenotype **(Figure 14 D, E White Dots)** except the epidermis of *AtEPF1pro::AtEPF1* in *epf1* which rescued *epf1* mutant phenotype **(Figure 14 A)**.

We also performed confocal analysis for grass *EPF2*-like genes to check if Bd/TaEPF2 homolog (*AtEPF1pro*:*BdEPF2* and At*EPF1pro::TaEPF2*) can compliment *epf1* mutant phenotype. We reported that none of EPF2-like homolog (*AtEPF1pro*:*:BdEPF2* and At*EPF1pro::TaEPF2*) was able to rescue *Arabidopsis epf1* phenotypic defects and showed a phenotype of paired stomata **(Figure 14 E, G, White dots).**

Our quantitative analysis also showed that our cross complementation lines of both *BdEPF1/2* and *TaEPF1/2* (*EPF1pro: BdEPF1/2* and *EPF1pro: TaEPF1/2)* homologs under *AtEPF1* native promotor could not compliment *epf1* background phenotype and possessed paired stomatal phenotype like *epf1* knockout mutant **(Figure 14 H).** Only, expression of our control i.e. *EPF1:AtEPF1* in *epf1* resulted into disappearance of paired stomata as in Columbia wild type **(Figure 14 H)**. Altogether, these results suggested that these *EPF1/EPF2*-like genes cannot replace the function of *AtEPF1* in *Arabidopsis.*

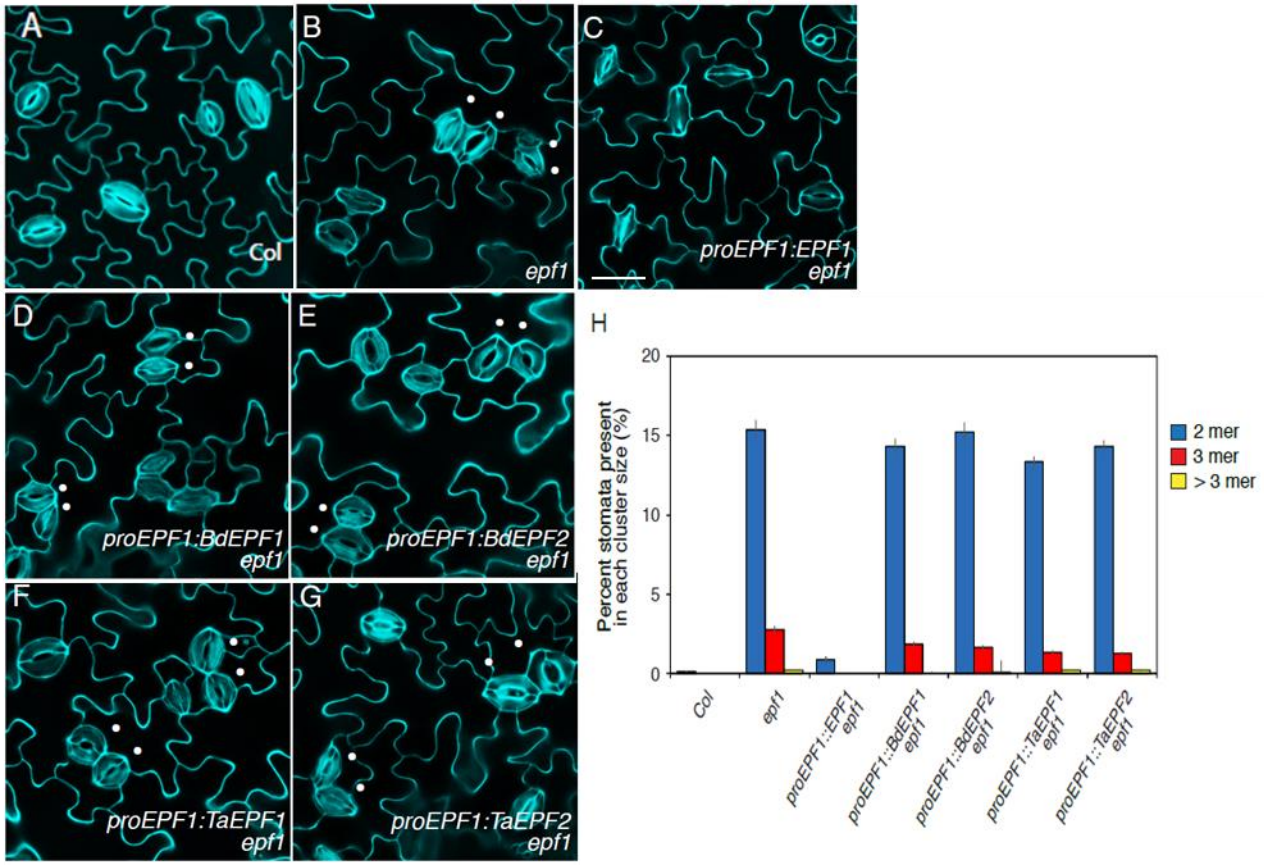

Figure 14. Cross-complementation analysis of two monocot *EPF1/EPF2* homologous genes in *Arabidopsis epf1* mutant

(A-G) Representative confocal images of 10-days-old abaxial cotyledons of the following genotypes: wild type Col (A), *epf1* (B), *EPF1pro: AtEPF1* (C), *EPF1pro: BdEPF1* (D), *EPF1pro: BdEPF2* (E), *EPF1pro: TaEPF1* (F) and *EPF1pro:TaEPF2*. Expression of *AtEPF1*, but not any of grass EPF1/2-like genes, driven by *Arabidopsis EPF1* promoter rescues the stomatal pairing (dots) of *Arabidopsis epf1* mutant. All confocal images were taken under the same magnification. Scale bars, 30 μm.

(H) Percentage stomata present in each cluster size (in %) in the *epf1* mutant and *epf1* expressing *AtEPF1* and *EPF1/2*-like genes in *Brachypodium* and wheat. Blue columns show 2mer, Red columns show 3mer and yellow columns show more than 3mer. *n* = 15-17 for each genotype. The experiments were repeated three times with similar results. Bars, means. Error bars, SE.

3.3.2. Grass EPF1/EPF2 homolog was proficient to complement the epidermal phenotypes of *Arabidopsis epf2* mutants

We next examined whether *EPF1/2*-like genes from two monocot species, wheat and *Brachypodium* can complement the epidermal phenotypes of *epf2*, excessive entry divisions resulting in significantly increased non-stomatal cell density (**Figure 15 B)**.

To do so, we performed epidermal phenotypic analysis of all complementation lines expressing *EPF1* and *EPF2* like grass homolog in *epf2* mutant background (*AtEPF2pro::BdEPF2, AtEPF2pro::BdEPF2, AtEPF2pro::TaEPF2,* and *AtEPF2pro::TaEPF1*). Similar to *AtEPF2pro::AtEPF2* in *epf2* **(Figure 15 C)**, expression of all grass *EPF1* and *EPF2* homologs driven by the endogenous *AtEPF2* promoter (*AtEPF2pro::BdEPF2, AtEPF2pro::BdEPF1, AtEPF2pro::TaEPF2*, and *AtEPF2pro::TaEPF1*) significantly rescued the epidermal phenotype of *epf2* mutant **(Figure 15 C, E, G)** which also supports our conclusion based on overexpression analyses.

We also wanted to quantify and compare the number of non-stomatal cells in our grass EPF1/2 complementation lines as compare to *epf2* loss of function mutant. Analysis of non-stomatal cell density (number of non-stomatal epidermal per mm^2) revealed that except *epf2* loss of function mutant, all our cross complimented constructs, *EPF2pro::BdEPF1/2*, *EPF2pro::TaEPF1/2* and control, *EPF2pro::AtEPF2* had a significant reduction in non-stomatal cell density **(Figure 15 H)**. Taken together, our observations indicate that all *EPF1/EPF2* homologs from wheat and its relative, grass model organism, *Brachypodium* can substitute AtEPF2 peptide, but they cannot replace the function of AtEPF1 in *Arabidopsis*.

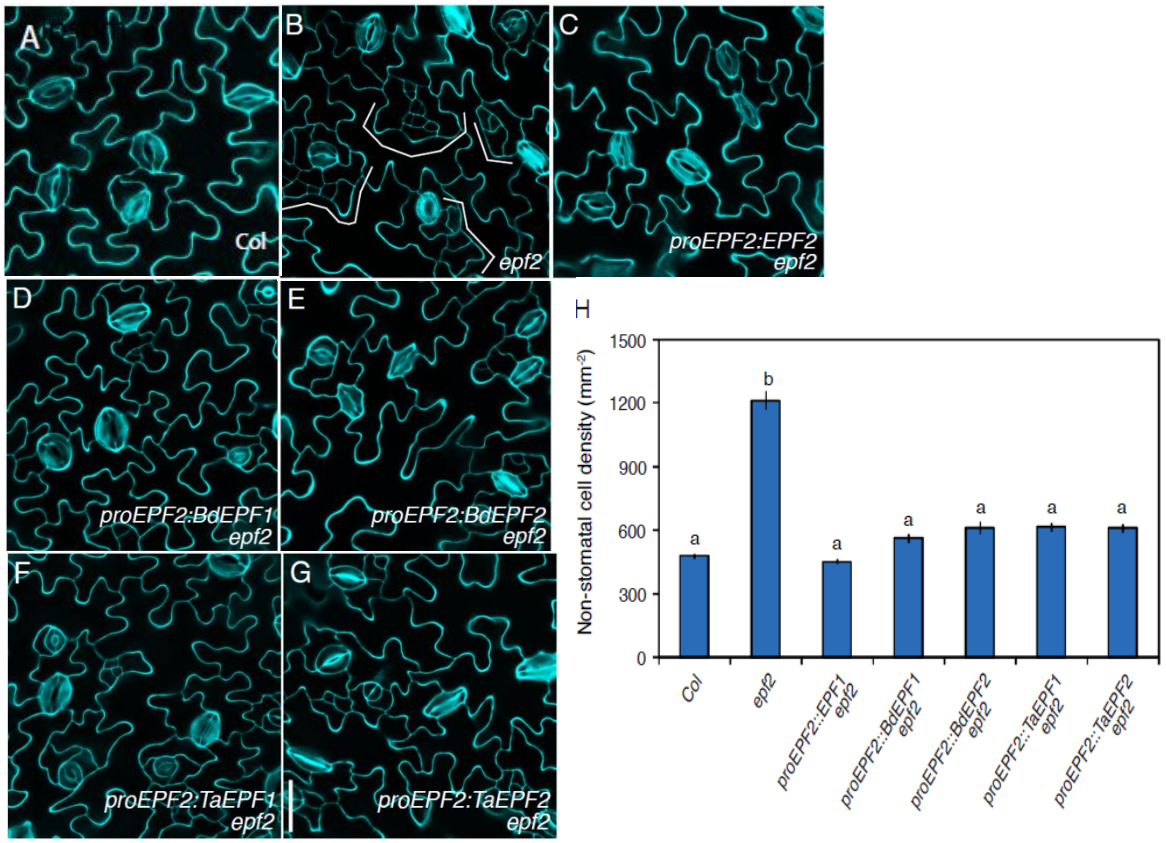

Figure 15. Complementation of *Arabidopsis epf2* mutants by grass *EPF1/EPF2* homologs

(A-G) Representative confocal images of 10-days-old abaxial cotyledons of the following genotypes: wild type Col (A), *epf2* (B), *EPF2pro: AtEPF2* (C), *EPF2pro: BdEPF1* (D), *EPF2pro: BdEPF2* (E), *EPF2pro:TaEPF1* (F) and *EPF2pro:TaEPF2*. The *epf2* knockout mutant, showed stomatal development defects (more stomata and small arrested cells (brackets; B). Excessive entry divisions (brackets), typical phenotype of *Arabidopsis epf2* mutant were complemented by *AtEPF2* as well as grass *EPF1/2*-like genes, which were expressed under the control of *Arabidopsis EPF2* promoter. all confocal images were taken under the same magnification. Scale bars, 30 μm.

(H) Non-stomatal epidermal cell density ((number of non-stomatal epidermal per mm^2) of 10-day-old abaxial cotyledons of *epf2* mutant and *epf2* expressing *AtEPF2* and grass *EPF1/2* homologs. Genotypes with no significantly different phenotypes were grouped together with the same letter ($P < 0.05$, Tukey's HSD test after one-way ANOVA). n = 15–17 for each genotype. The experiments were repeated three times with similar results. Bars, means. Error bars, SE.

3.4 Exogenous application of mature grass EPF (MEPF) peptides triggers stomatal developmental defects in *Brachypodium* seedlings

Overexpression and cross-species complementation experiments indicated that there are two copies of stomatal EPF homologs in wheat and *Brachypodium* that behave like *AtEPF2* and *AtSTOMAGEN*, respectively, when they are expressed in *Arabidopsis*. To gain insight into the role of these grass EPF peptides in regulating grass stomatal development, which have different stomatal morphologies and patterns in comparison to *Arabidopsis*, we next examined the phenotypic effects of *Brachypodium* seedlings (Bd21-3) treated with bioactive mature EPF peptides, MBdEPF1/2-1, MBdEPF1/2-2, and MBdSTOMAGEN-1. MBdSTOMAGEN-2 was excluded from the analyses because it has the same effect as BdSTOMAGEN-1 in stomatal development when they are expressed in *Arabidopsis*.

Our work focused mainly on EPF peptides from the model grass organism *Brachypodium* because of the similarity in the phenotypes produced by stomatal EPF homologs from wheat and *Brachypodium*. We first produced C-terminal predicted mature forms of recombinant MBdEPF1 (91 amino acids), MBdEPF2 (83 amino acids), and chemically synthesized MBdSTOMAGEN-1 (45 amino acids) peptides based on the protocol we developed for *Arabidopsis* EPFs in previous study (Lee *et al*., 2012). After refolding, we applied these bioactive grass EPF peptides to *Brachypodium* wild type, Bd21-3 seedlings to investigate effects of these *Brachypodium* EPF peptides in grasses. Further, to check the effect of mature peptides, leaf epidermal phenotype of *Brachypodium* seedlings treated with MBdEPF1, MBdEPF2 and MBdSTOMAGEN were analyzed at 7-9 dpg.

As shown in Figure16A, the grass leaf epidermis in wild-type (mock-treated Bd21-3) seedlings generated orderly patterned stomata in specific cell files typically located 1–2 cells away from veins, unlike the scattered pattern of stomata in dicot *Arabidopsis* leaves. Application of bioactive, MBdEPF1 and MBdEPF2 peptide solution inhibited stomatal development, while MBdSTOMAGEN-1 treatment promoted stomatal density and stomatal clustering in the stomatal cell files of *Brachypodium* leaf epidermis **(Figure 16 B-E)**. These results suggested that orthologs of AtEPF2 and AtSTOMAGEN may also be involved in regulating stomatal initiation with opposing activities in monocots.

However, unlike overexpressed *Arabidopsis EPF1* and *EPF2*, we found that application of either MBdEPF1 or MBdEPF2 peptide failed to induce any obvious change to other non-stomatal

epidermal cells, such as silica cells in veins and hair cells, although the generation of stomata or stomatal precursors was completely blocked. Hair cells, instead of stomata, were generated in stomatal cell files of the *Brachypodium* epidermis **(Figure 16 B, C, F)**, suggesting that the default cell fate of smaller cells of asymmetric divisions in entire epidermal lineages of grass is not affected by the application of *Brachypodium* EPF peptides, MBdEPF1 and MBdEPF2.

On the other hand, *Brachypodium* seedlings treated with MBdSTOMAGEN-1 displayed variability in the strength of phenotype, and the seedlings showing strongest epidermal phenotypes exhibited some unusual SC morphologies **(Figure 16 G; arrowheads)** and ectopic stomatal rows in addition to increased stomatal density and stomatal patterning defects. In addition, MBdSTOMAGEN-1 also showed some paired guard cells spanned by only one subsidiary cell which is very unlikely in wild type *Brachypodium* seedlings **(Figure 16 D; dots, G;arrowheads)**. Taking these results together, our data indicate that grass EPF peptides MBdEPF1/2 and BdSTOMAGEN are key secreted signaling peptides with opposing functions to control grass stomatal initiation. Also, function of monocot MEPF1/2 homologs are much more like *Arabidopsis* EPF2 than EPF1.

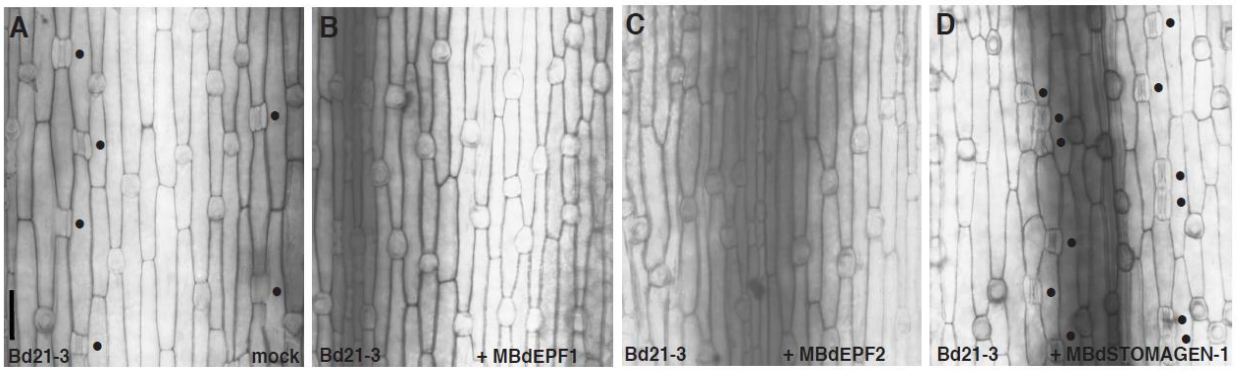
A
Bd21-3
mock
B
Bd21-3
+ MBdEPF1
C
Bd21-3
+ MBdEPF2
D
Bd21-3
+ MBdSTOMAGEN-1

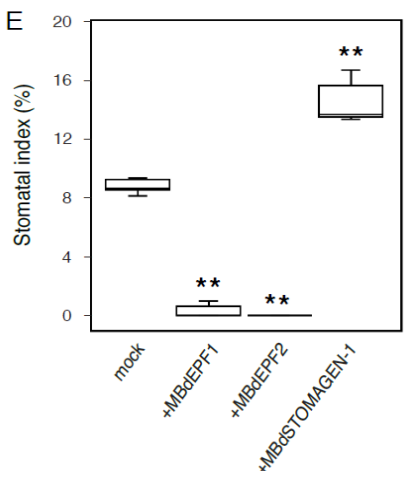
E
Stomatal index (%)
20
16
12
8
4
0
**
**
**
mock
+MBdEPF1
+MBdEPF2
+MBdSTOMAGEN-1

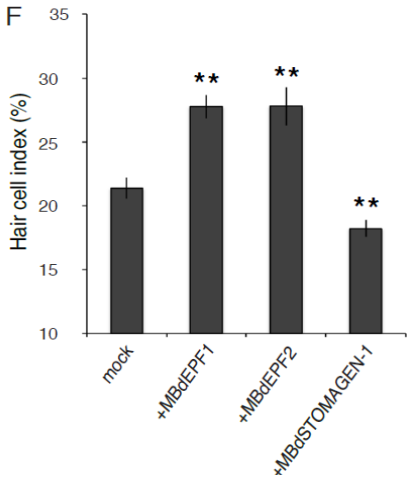
F
Hair cell index (%)
35
30
25
20
15
10
**
**
**
mock
+MBdEPF1
+MBdEPF2
+MBdSTOMAGEN-1

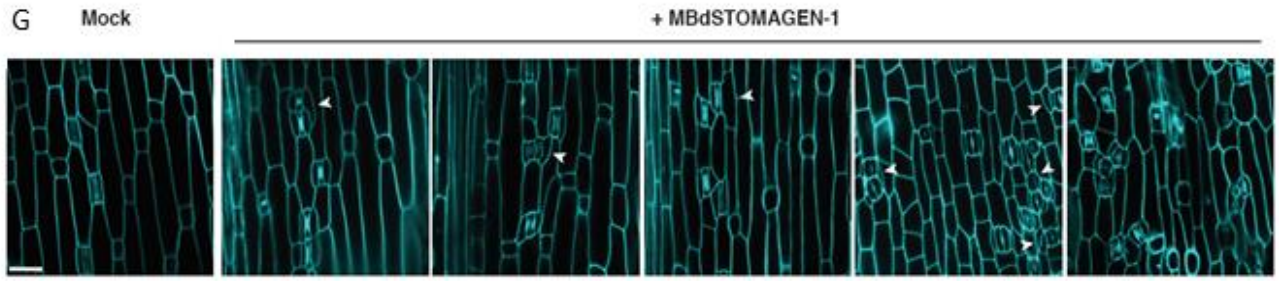
G
Mock
+ MBdSTOMAGEN-1

Figure 16. MBdEPF1/2 restricts stomatal development while MBdSTOMAGEN does opposite in Bd21-3 seedlings (*Brachypodium distachyon*)

(A-C) Images of the abaxial epidermis of 5-7dpg first leaf of 'Bd21-3' control (A), MBdEPF1(B), MBdEPF2(C) and MBdSTOMAGEN(D) treated seedlings. All images were taken at 20X, Z1. Scale bars, 30 μm.

(E) Quantitative analysis of 10-days-old abaxial cotyledon epidermis. Stomatal index (SI) expressed as the percentage of the number of stomata to the total number of epidermal cells. Asterisks indicate significant difference in SI compared with data from wild type plants (Student's t-test with P values of < 0.0001). *n* = 8-10 for each genotype. The experiments were repeated three times with similar results. Bars, means. Error bars, SE.

(F) Quantitative analysis of 10-days-old abaxial cotyledon epidermis. Hair cell density (HSD) of MBdEPF1, MBdEPF2 and MBdSTOAMGEN-1 treated *Brachypodium* seedlings compared to that of WT, Bd21-3. HSD expressed as the ratio of hair cells to of all other stomatal and non-stomatal epidermal cells in a fixed area. Asterisks above the columns indicate significant difference compared with data from Mock, Bd21-3 (Student's t-test with P values of < 0.0001). *n* = 8-10 for each genotype. The experiments were repeated three times with similar results. Bars, means. Error bars, SE.

(G) Confocal images of the abaxial epidermis of 5-7 dpg first leaf of MBdSTOMAGEN-1 treated seedlings showing different abnormal SC morphologies (While arrow heads) as compare to mock. All images were taken at 40X, Z1. Scale bars, 30 μm.

4. Discussion:

Grasses are very important plant group for food, feed and energy production. Among this group, cereal crops hold critical importance in terms of feeding livestock. According to today's climate changing scenario, it is very important to find newer techniques for improved monocot growth and yield. Also, previous studies of dicot model plant (*Arabidopsis thaliana*) showed that, under normal and drought conditions, altering stomatal density plays crucial role in determining plant health and biomass production (Franks *et al*., 2015). Frank *et al*, (2015) produced *EPF2OE* constructs and proved that upon genetic alteration of *EPF2*, a well known negative stomatal regulator, plants with higher water utilization efficiency can be produced.

On the basis of genes identified in *Arabidopsis*, researchers are also trying to discover novel genes in grasses which can assist in stomatal development process. For instance, grasses also use specific bHLH transcriptional factor and MAPKKK orthologs of *Arabidopsis* for different cell transition stages (Raissig *et al*., 2016; Raissig *et al*., 2017; Liu *et al*., 2009 and Abrash *et al*., 2018). Another recent study in cereals showed that genetic alteration of different grass stomatal orthologs can produce crops (*Hordeum vulgare*) with better WUE under future drought or water restricted conditions (Hepworth *et al.*, 2017).

In the present study, we chose to identify and characterize small signaling peptide; EPF homologous in different cereal crops. We considered 3 well explored *Arabidopsis* stomatal EPFs; *EPF1* (Hunt and Gray, 2009), *EPF2* (Hara *et al.*, 2007) and *STOMAGEN* (Hunt and Gray, 2010; Sugano *et al.*, 2010; Shimada *et al.*, 2011) as our references. So that, prior knowledge of characterized *Arabidopsis* stomatal EPFs can be used to predict and compare function of monocot stomatal EPF homologous genes.

4.1 Stomatal signaling peptide homologs exist in different cereal crops

In the present study, stomatal EPFs homologs in several crops were identified and we characterized *Bd/TaEPF1*, *Bd/TaEPF2*, *Bd/TaSTOMAGEN* homologs in *Brachypodium* and *Triticum aestivum.* We have found that 2 copies of monocot *STOMAGEN* homologous gene in both *Brachypodium* and *Triticum*. While in *Arabidopsis*, only one copy of *STOMAGEN* exists. Similar findings were observed by Hepworth *et al*, (2017) who claimed that all of monocots they checked for EPF homologs possessed two *STOMAGEN* like homologous genes and it could happen because of duplication of a single gene resulting in two individual genes. Some other group also identified putative stomatal EPFs homologous in some crops such as Rice (Lu *et al.*, 2019), and other woody plants like poplar (Wang *et al.*, 2016).

4.2 Function of positive stomatal EPF peptides appears to be conserved in different plant species

STOMAGEN is discovered as a positive regulator of stomata development in *Arabidopsis* (Hunt and Gray, 2010). Unlike other stomatal EPFs, it expresses in inner mesophyll tissues and result in increased stomatal density and clustering (Sugano *et al.*, 2010; Hunt and Gray, 2010; Shimada *et al.*, 2011). In the present study, our inducible overexpression analysis (Both phenotypic and quantitative) showed that both *Bd/TaSTOMAGEN-1* and *Bd/TaSTOMAGEN-2* behaves like orthologs of *AtSTOMAGEN* and showed excessive number of stomata as clusters upon induction with estradiol **(Figure 6 D, E, F, K, L)**. Also, exogenous application of bioactive *Brachypodium* STOMAGEN-1 (MBdSTOMAGEN-1) showed clustered stomata in *Brachypodium* wild type, Bd21-3 seedlings **(Figure 16 D)**. This gives a strong idea that grass STOMAGEN is an ortholog of *Arabidopsis* STOMAGEN and acts as a positive stomatal regulator in grasses.

Recently, a research group (Yin *et al.*, 2017) had identified rice *STOMAGEN* ortholog by generating CRISPER/Cas9 knockout lines. They showed that *OsSTOMAGEN* knockout lines resulted in plants with diminished stomatal density like in *AtSTOMAGEN* knockdown lines and overexpression lines produced excessive clustered stomata (Hunt and Gray, 2010). These previous

findings also support our hypothesis of conservation of *STOMAGEN* function in dicots and grasses.

4.3 Negative stomatal EPF function may diverge in different plant species

Regulation of stomatal initiation and differentiation by two important stomatal EPFs, *EPF1* and *EPF2* in *Arabidopsis* shows that overexpression of these two genes result in a pavement cell devoid of stomata. In addition, *AtEPF1OE* shows small arrested cell in its epidermis. In the present study, we applied this approach for monocot stomatal EPFs and generated overexpression lines to predict their function in monocots. Our findings suggested overexpressed *Bd/TaEPF2* homologous were able to reduce stomatal density and showed a phenotype like *AtEPF2* overexpression (Hara *et al.*, 2009).

However, our hypothesis illustrated functional deviation in *Bd/TaEPF1* homologous because of absence of small arrested looking like cells **(Figure 11 E, F)** which was not t case in *AtEPF1OE* **(Figure 11 D)**. But as like dicot *EPF1*, *Bd/TaEPF1* also showed negative stomatal regulation by decreasing stomatal density. We also reconfirmed these results in *Brachypodium* by generating and treating Bd21-3 seedlings with bioactive MBdEPF1 and MBdEPF2 exogenously **(Figure 16 B, C)**. This gives us idea that these two monocot homologous genes hold a degree of conservation, but *Bd/TaEPF1* and *Bd/TaEPF2* behaves like *Arabidopsis EPF2* gene as compare to *AtEPF1*.

This could be possible because grasses' stomatal development does not possess meristemoids where *EPF1* acts upon specifically in dicot *Arabidopsis.* Grasses have one asymmetric division which leads to formation of a GMC and pavement cell (Stebbins and Jain, 1960; Hepworth *et al*., 2017). Whereas, in *Arabidopsis* meristemoids undergoes multiple amplifying asymmetric divisions (Serna, 2009). This can be a reason that both *Brachypodium* and Wheat *EPF1/EPF2* behave like *AtEPF2* and controls entry divisions.

Functionaly analysis of EPF peptides have also been conducted on different crops and woody plants to see altered stomatal density effect on plant yield with better WUE. One of them is overexpression of *EPF1* homolog, *PdEPF1* in poplar (Wang *et al*., 2016), a woody deciduous

plant showed great reduction in stomatal density. In return, *PdEPF1OE* plants resulted in improved water utilization efficiency under drought condition as compare to control plants.

Dunn and Hunt (2019) also demonstrated effect of wheat *EPF1/2* like genes by creating transgenic wheat *EPF1/2* overexpression lines. They also observed reduction in stomatal density in plant overexpressing *TaEPF1/2* genes and plants with nil or very less stomatal density showed better water efficiency under controlled conditions.

Hepworth *et al*, (2017) showed some EPF ortholog study results in barley, where they observed contradictory results from our EPF homologs study. They proposed that function of *HvEPF1/2* homologs are more like *AtEPF1* because they found small arrested cells which could not differentiate into A GMC in barley plants overexpressing *HvEPF1*. Additionally, *Hordeum vulgare* carrying *HvEPF1* overexpressed transgene also showed great reduction in stomatal density and showed better yield with plants growing in water restricted conditions.

It might be possible to observe different results in different crops. Also, both *EPF2* and *EPF1* genes are very close to each other so they might have some overlapping and divergent function in various grass species.

In this study, we uncovered function of stomatal EPF homologs in two monocots, *Brachypodium distachyon* and *Triticum aestivum*. We found that both *Bd/TaEPF1* and *Bd/TaEPF2* homologous genes behave like *AtEPF2*. In conclusion, grasses exhibit stomatal EPF homologs alike dicots with a degree of functional divergence between two species. With the help of such knowledge, researchers can manipulate different crop's stomatal gene and optimise field work conditions to see the effect. Further exploration about EPFs can be great asset for drought resistant crop with more productivity to fight against upcoming water scarcity and more food demand.

In future, biochemical interaction studies can be an asset for better understanding of grasses stomatal EPF homologous genes that how they regulate signaling pathways by interacting with different cell surface receptors. In dicots, EPF1 serves as a ligand for ERL1 and control proper stomatal spacing divisions. Whereas EPF2 receives signals from cell surface ER receptor and collectively they regulate stomatal initiation process (Lee *et al*., 2012). Identification of stomatal

receptors for grass EPFs will help us to better control stomatal differentiation at different development stage in monocots.

5. References:

1. **Abrash E, Anleu Gil MX, Matos JL, Bergmann DC**. (2018) Conservation and divergence of YODA MAPKKK function in regulation of grass epidermal patterning. Development **145**: dev165860

2. **Abrash EB, Davies KA, Bergmann DC**. (2011) Generation of signaling specificity in Arabidopsis by spatially restricted buffering of ligandreceptor interactions. Plant Cell **23**:2864–2879.

3. **Adams, ML, Lombi E, Zhao FJ, McGrath SP**. (2002) Evidence of low selenium concentrations in UK bread-making wheat grain. Journal of the Science of Food and Agriculture **82**:1160-1165.

4. **Bergmann DC, Sack FD**. (2007) Stomatal development. Annu. Rev. Plant. Biol **58**:163-181.

5. **Bergmann DC, Lukowitz W, Somerville CR**. (2004) Stomatal development and pattern controlled by a MAPKK kinase. Science **304**:1494–1497.

6. **Bessho-Uehara K, Wang DR, Furuta T, Minami A, Nagai K, Gamuyao R, Asano K, Angeles-Shim RB, Shimizu Y, Ayano M**, et al. (2016) Loss of function at *RAE2*, a previously unidentified EPFL, is required for awn lessness in cultivated Asian rice. Proc Natl Acad Sci USA **113**:8969–8974.

7. **Bhave NS, Veley KM, Nadeau JA, Lucas JR, Bhave SL, Sack FD**. (2009) TOO MANY MOUTHS promote cell fate progression in stomatal development of *Arabidopsis* stems. Planta **229**:357–367.

8. **Breiman A, Graur D**. (1995) Wheat Evaluation. Israel Journal of Plant Sciences **43**:58-95.

9. **Briggle LW, Reitz LP**. (1963) Classification of Triticum species and of wheat varieties grown in the United States. United States Department of Agriculture. Technical Bulletin, 1278.

10. **Caine RS, Yin X, Sloan J, Harrison EL, Mohammed U, Fulton T, Biswal AK, Dionora J, Chater CC, Coe RA, Bandyopadhyay A, Murchie EH, Swarup R, Gray JE.** (2018) Rice with reduced stomatal density conserves water and has improved drought tolerance under future climate conditions. New Phytologist **221**:371-384.

11. **Casson S, Gray JE**. (2007) Influence of environmental factors on stomatal development. New Phytol. **178**:9–23.

12. **Clough SJ, Bent AF**. (1998) Floral dip: a simplified method for *Agrobacterium*-mediated transformation of *Arabidopsis thaliana*. Plant J. **16**:735-743.

13. **Colcombet J, Hirt H**. (2008) *Arabidopsis* MAPKs: a complex signaling network involved in multiple biological processes. Biochem. J. **413**:217-226.

14. **Croxdale J**. (1998) Stomatal patterning in monocotyledons: Tradescantia as a model system. Journal of Experimental Botany **49**:279-292.

15. **Dohlman HG, Thorner JW**. (2001) Regulation of G protein-initiated signal transduction in yeast: paradigms and principles. Ann. Rev. Biochem **70**: 703-754.

16. **Dunn J, Hunt L, Afsharinafar M, Meselmani M Al, Mitchell A, Howells R, Wallington E, Fleming AJ, Gray JE**. (2019) Reduced stomatal density in bread wheat leads to increased water-use efficiency. Journal of Experimental Botany **70**:4737–4747.

17. **Edwards K, Johnstone C, Thompson C**. (1991) A simple and rapid method for the preparation of plant genomic DNA for PCR analysis. Nucleic acids research **19**:1349.

18. **FAOSTAT**. (2017) Food and Agriculture Organization of the United Nations. Available online at: https://data.worldbank.org/indicator/AG.PRD.CREL.MT.

19. **FAOSTAT**. (2020) Food and Agriculture Organization of the United Nations. Available online at: http://faostat3.fao.org/download/Q/QC/E (Accessed May 2015).

20. **Franks PJW, Doheny Adams T, Britton Harper ZJ, Gray JE**. (2015) Increasing water-use efficiency directly through genetic manipulation of stomatal density. New Phytologist **207**:188–195.

21. **Gallagher K, Smith LG**. (2000) Roles for polarity and nuclear determinants in specifying daughter cell fates after an asymmetric cell division in the maize leaf. Curr. Biol. **10**:1229–1232.

22. **Gao X, Guo Y**. (2012) CLE peptides in plants: proteolytic processing, structure-activity relationship, and ligand-receptor interaction. J. Integ. Plant Biol **54**:738-745.

23. **Geisler M, Nadeau J, Sack FD, Nadeau J, Sack FD, Sack FD**. (2000) Oriented asymmetric divisions that generate the stomatal spacing pattern in *Arabidopsis* are disrupted by the too many mouths mutation. Plant Cell **12**:2075–2086.

24. **Godfray HCJ, Beddington JR, Crute IR, Haddad L, Lawrence D, Muir JF, Pretty J, Robinson S, Thomas SM, Toulmin C** (2010) Food security: the challenge of feeding 9 billion people. Science **327**:812–818.

25. **Gudesblat GE, Schneider-Pizoń J, Betti C, Mayerhofer J, Vanhoutte I, van Dongen W, Boeren S, Zhiponova M, de Vries S, Jonak C**. *et al*. (2012) *SPEECHLESS* integrates brassinosteroid and stomata signaling pathways. Nat. Cell Biol. **14**:548-554.

26. **Guseman JM, Lee JS, Bogenschutz NL, Peterson KM, Virata RE, Xie B, Kanaoka MM, Hong Z, Torii KU**. (2010) Dysregulation of cell-to-cell connectivity and stomatal patterning by loss-of-function mutation in Arabidopsis CHORUS (GLUCAN SYNTHASE-LIKE 8). Development **137**:1731–1741.

27. **Haleem, Abd-El-SHM, Reham MA, Mohamed SMS, Abdel-Aal ESM, Sosulski FW, Hucl P**. (1998) Origins, characteristics and potentials of ancient wheat. Cereal Foods World **43**:708–715.

28. **Hara K, Kajita R, Torii KU, Bergmann DC, Kakimoto T**. (2007) The secretory peptide gene *EPF1* enforces the stomatal one-cell-spacing rule. Genes **21**:1720–1725.

29. **Hara K, Yokoo T, Kajita R, Onishi T, Yahata S, Peterson KM, Russinova E.** (2009) Epidermal cell density is autoregulated via a secretory peptide, EPIDERMAL PATTERNING FACTOR 2 in *Arabidopsis* leaves. Plant Cell Physiol **50**:1019–1031.

30. **Hepworth C, Hughes J, Dutton C, Dunn JA, Hunt L, Stephens J, Cameron D, Waugh R, Gray JE**. (2017) Reducing stomatal density in barley improves drought tolerance without impacting on yield. Plant Physiol. **174:**776–787.

31. **Hunt L, Bailey KJ, Gray JE**. (2010) The signaling peptide STOMAGEN is a positive regulator of stomatal development. New Phytol **186**:609-614.

32. **Hunt L, Gray JE**. (2009) The signaling peptide EPF2 controls asymmetric cell divisions during stomatal development. Curr Biol **19**:864-869.

33. **IPCC** (2014) Climate Change 2014: Synthesis Report. Pachauri RK, Meyer LA. (eds.) Contribution of Working Groups I, II and III to the Fifth Assessment Report of the Intergovernmental Panel on Climate Change. IPCC, Geneva, Switzerland, 151.

34. **Jackson SA**. (2016) Rice: The First Crop Genome. Rice (N Y) **9**:14. doi:10.1186/s12284-016-0087-4.

35. **Jarvis PG, Mansfield TA**. (1981) Stomatal physiology. Vol 8: Cambridge University Press.

36. **Kanoka MM, Pillitteri LJ, Fujii H, Yoshida Y, Bogenschutz NL, Takabayashi J, Zhu J.K, Torii KU.** (2008) SCREAM/ ICE1 and SCREAM2 specify three cell-state transitional steps leading to Arabidopsis stomatal differentiation. Plant Cell **20**:1775–1785

37. **Karamboulas C, Ailles L**. (2012) Developmental signaling pathways in cancer stem cells of solid tumors. Biochim. Biophys. Acta **1830**:2481-95.

38. **Kole C**. (2006) Cereals and Millets, Berlin; New York: Springer.

39. **Kondo T, Kajita R, Miyazaki A, Hokoyama M, Nakamura-Miura T, Mizuno S, Masuda Y, Irie K, Tanaka Y, Takada S, Kakimoto T, Sakagami Y**. (2010) Stomatal density is controlled by a mesophyll-derived signaling molecule. Plant Cell Physiol **51**:1-8.

40. **Kosentka PZ, Overholt A, Maradiaga R, Mitoubsi O, Shpak ED**. (2019) EPFL Signals in the Boundary Region of the SAM Restrict Its Size and Promote Leaf Initiation. Plant physiology **179**:265–279.

41. **Kumar P, Yadava RK, Gollen B, Kumar S, Verma RK, Yadav S**. (2011) Nutritional Contents and Medicinal Properties of Wheat: A Review. Life Sciences and Medicine Research.

42. **Kumar S, Stecher G, Tamura K**. (2016) MEGA7: Molecular Evolutionary Genetics Analysis Version 7.0 for Bigger Datasets, Molecular Biology and Evolution. **33**:1870–1874.

43. **Larkin JC, Marks MD, Nadeau J, Sack F**. (1997) Epidermal cell fate and patterning in leaves. Plant Cell **9**:1109-1120.

44. **Lee JS, Hnilova M, Maes M, Lin YCL, Putarjunan A, Han SK, Avila J, Torii KU**. (2015) Competitive binding of antagonistic peptides fine-tunes stomatal patterning. Nature **522**:439-443.

45. **Lee J, Kuroha T, Hnilova M, Khatayevich D, Kanaoka MM, McAbee JM, Sarikaya M, Tamerler C, Torii KU**. (2012) Direct interaction of ligand-receptor pairs specifying stomatal patterning. Genes Dev. **26**:126-136.

46. **Liu T, Ohashi-Ito K, Bergmann DC**. (2009) Orthologs of *Arabidopsis thaliana* stomatal bHLH genes and regulation of stomatal development in grasses. Development (Cambridge, England) **136**:2265–76.

47. **Lu J, He J, Zhou X, Zhong J, Li J, Liang Y-KK**. (2019) Homologous genes of epidermal patterning factor regulate stomatal development in rice. Journal of Plant Physiology **27**:234–235.

48. **MacAlister CA, Ohashi-Ito K, Bergmann DC**. (2007) Transcription factor control of asymmetric cell divisions that establish the stomatal lineage. Nature **445**:537–540.

49. **Nadeau JA, Sack FD**. (2002) Control of stomatal distribution on the *Arabidopsis* leaf surface. Science **296**:1697–1700.

50. **Ohashi-Ito K and Bergmann D.C**. (2006) *Arabidopsis* FAMA controls the final proliferation/differentiation switch during stomatal development. Plant Cell **18**:2493–2505.

51. **Ohki S, Takeuchi M, Mori M**. (2011) The NMR structure of *STOMAGEN* reveals the basis of stomatal density regulation by plant peptide hormones. Nat Commun **2**:512.

52. **Peterson KM, Rychel AL, Torii KU**. (2010) Out of the mouths of plants: molecular basis of the evolution and diversity of stomatal development. Plant Cell **22**:296-306.

53. **Pfaffl MW**. (2001) A new mathematical model for relative quantification in real-time RT-PCR. Nucleic Acids Res **29**: e45

54. **Pillitteri LJ, Dong J**. (2013) Stomatal development in *Arabidopsis*. The *Arabidopsis* book **11**: e0162.

55. **Pillitteri LJ, Sloan DB, Bogenschutz NL, Torii KU.** (2007) Termination of asymmetric cell division and differentiation of stomata. Nature **445**:501–505.

56. **Pillitteri, LJ, Torii KU**. (2012) Mechanisms of stomatal development. Annu. Rev. Plant Biol. **63**:591–614.

57. **Portwood JL 2nd, Woodhouse MR, Cannon EK, Gardiner JM, Harper LC, Schaeffer ML, Walsh JR, Sen TZ, Cho KT, Schott DA, Braun BL, Dietze M, Dunfee B, Elsik CG, Manchanda N, Coe E, Sachs M, Stinard P, Tolbert J, Zimmerman S, Andorf CM**. (2019) MaizeGDB: the maize multi-genome genetics and genomics database. Nucleic acids research, **47**:1146–D1154.

58. **Posner ES**. (2000) Wheat. In: Kulp, KEA. (ed.) Handbook of Cereal Science and Technology. New York: Marcel Dekker, 1-29.

59. **Raissig MT, AbrashE, Bettadapur A, Vogel JP, Bergmann DC**. (2016) Grasses use an alternatively wired *bHLH* transcription factor network to establish stomatal identity. Proc. Natl. Acad. Sci. U.S.A. **113**:8326–8331.

60. **Raissig MT, Matos JL, Gil MXA, Kornfeld A, Bettadapur A, Abrash E, Allison HR, Badgley G, Vogel JP, Berry JA, Bergmann DC**. (2017) Mobile *MUTE* specifies subsidiary cells to build physiologically improved grass stomata. Science **355**:1215–1218.

61. **Raschke K**. (1979) Movements of stomata. In Physiology of Movements, Encyclopedia of Plant Physiology **7**:383–441.

62. **Richardson LGL, Torii KU**. (2013) Take a deep breath: peptide signaling in stomatal patterning and differentiation. Journal of Experimental Botany **64**:5243–5251.

63. **Rowe MH, Bergmann DC**. (2010) Complex signals for simple cells: the expanding ranks of signals and receptors guiding stomatal development. Current opinion in plant biology **13**:548-555.

64. **Sachs T**. (1991) In Pattern formation in plant tissues (Cambridge University Press), 205-206.

65. **Scholthof KBG, Irigoyen S, Catalan P, Mandadi KK**. (2018) *Brachypodium*: A monocot grass model genus for plant biology. Plant Cell **30**:1673–1694.

66. **Serna L**. (2009) Cell fate transitions during stomatal development. Bioassays **31**:865-873.

67. **Serna L, Torres-Contreras J, Fenoll C**. (2002) Specification of stomatal fate in *Arabidopsis*: evidence for cellular interactions. New Phytologist **153**:399–404.

68. **Shaw LM, Turner AS, Laurie DA**. (2012) The impact of photoperiod insensitive Ppd-1a mutations on the photoperiod pathway across the three genomes of hexaploid wheat (*Triticum aestivum*). Plant J **71**:71-84.

69. **Shewry PR**. (2009) Wheat. Journal of Experimental Botany **60**:1537-1553.

70. **Shewry, PR**. (2007) Improving the protein content and composition of cereal grain. Journal of Cereal Science **46**:239–250.

71. **Shimada T, Sugano SS, Hara-Nishimura I**. (2011) Positive and negative peptide signals control stomatal density. Cell Mol Life Sci **68**:2081–2088.

72. **Shpak ED, Lakeman MB, Torii KU**. (2003) Dominant-negative receptor uncovers redundancy in the *Arabidopsis ERECTA* Leucine rich repeat receptor-like kinase signaling pathway that regulates organ shape. Plant Cell **15**:1095-1110.

73. **Singh H, Singh AK**. (2007) Energy consumption pattern of wheat production in India. Energy **32**:1848-1854.

74. **Smith LG, Zhang X, Facette M, Humphries JA, Shen Z, Park Y, Sutimantanapi D, Sylvester AW, Briggs SP**. (2012) Identification of *PAN2* by quantitative proteomics as a leucine-rich repeat-receptor-like kinase acting upstream of *PAN1* to polarize cell division in maize. Plant Cell **24**: 4577–4589.

75. **Stebbins GL, Shah SS**. (1960) Developmental studies of cell differentiation in the epidermis of monocotyledons: II. Cytological features of stomatal development in the Gramineae. Dev. Biol. **2**:477-500.

76. **Sugano SS, Shimada T, Imai Y, Okawa K, Tamai A, Mori M, Hara- Nishimura I**. (2010) *STOMAGEN* positively regulates stomatal density in *Arabidopsis*. Nature **463**:241-244.

77. **Takata N, Yokota K, Ohki S, Mori M, Taniguchi T, Kurita M**. (2013) Evolutionary relationship and structural characterization of the EPF/ EPFL gene family. PLoS One **8**: e65183.

78. **Tameshige T, Okamoto S, Lee JS, Aida M, Tasaka M, Torii KU, Uchida N**. (2016) A secreted peptide and its receptors shape the auxin response pattern and leaf margin morphogenesis. Curr Biol **26**:2478–2485.

79. **Torii KU**. (2012) Mix-and-match: ligand-receptor pairs in stomatal development and beyond. Trends Plant Sci **17**:711–719.

80. **Torii KU, Mitsukawa N, Oosumi T, Matsuura Y, Yokoyama R, Whittier RF, Komeda Y**. (1996) The *Arabidopsis ERECTA* gene encodes a putative receptor protein kinase with extracellular leucine rich repeats. Plant Cell **8**:735-746.

81. **Uchida N, Lee JS, Horst RJ, Lai HH, Kajita R, Kakimoto T, Tasaka M, Torii KU**. (2012) Regulation of inflorescence architecture by inter tissue layer ligand–receptor communication between endodermis and phloem. Proceedings of the National Academy of Sciences, USA **109**:6337–6342.

82. **Whelan S, Goldman N.** (2001) A general empirical model of protein evolution derived from multiple protein families using a maximum-likelihood approach. Mol Biol Evol **18**:691-699.

83. **Wang C, Liu S, Dong Y, Zhao Y, Geng A, Xia X, Yin W**. (2016) *PdEPF1* regulate water-use efficiency and drought tolerance by modulating stomatal density in poplar. Plant Biotechnol. J. **14**:849–860.

84. **Wang H, Guo S, Qiao X, Guo J, Li Z, Zhou Y, Bai S, Gao Z, Wang D, Wang P, et al**. (2019) *BZU2/ZmMUTE* controls symmetrical division of guard mother cell and specifies neighbor cell fate in maize (S Hake, Ed.). PLOS Genetics **15**: e1008377.

85. **Wang H, Ngwenyama N, Liu Y, Walker J, Zhang S**. (2007) Stomatal development and patterning are regulated by environmentally responsive mitogen-activated protein kinases in Arabidopsis. The Plant Cell **19**:63-73.

86. **Wang Q, Hasson A, Rossmann S, Theres K**. (2016) Divide et impera: Boundaries shape the plant body and initiate new meristems. New Phytol **209**: 485–498.

87. **Yin X, Biswal AK, Dionora J, Perdigon KM, Balahadia CP, Mazumdar S, Chater C, Lin H-C, Coe RA, Kretzschmar T, Gray JE, Paul W, Bandyopadhyay, A.** (2017) CRISPR-Cas9 and CRISPR-Cpf1 mediated targeting of a stomatal developmental gene *STOMAGEN* in rice. Plant Cell Reports **36**:745–757.

88. **Zuo, Niu QW, Chua NH**. (2000) Technical advance: An estrogen receptor-based trans activator XVE mediates highly inducible gene expression in transgenic plants. Plant J **24**:265-273.